Development 139, 3752-3763 (2012) doi:10.1242/dev.074203


# Multifaceted roles of PTEN and TSC orchestrate growth and differentiation of *Drosophila* blood progenitors

**Michelle Dragojlovic-Munther[1] and Julian A. Martinez-Agosto[2,*]**

## SUMMARY

The innate plasticity of hematopoietic progenitors is tightly regulated to supply blood cells during normal hematopoiesis and in response to stress or infection. We demonstrate that in the *Drosophila* lymph gland (LG) the tumor suppressors TSC and PTEN control blood progenitor proliferation through a common TOR- and 4EBP-dependent pathway. *Tsc2* or *Pten* deficiency in progenitors increases TOR signaling and causes LG overgrowth by increasing the number of actively dividing cells that accumulate high levels of phosphorylated (p) 4EBP during a critical window of growth. These phenotypes are associated with increased reactive oxygen species (ROS) levels in the LG, and scavenging ROS in progenitors is sufficient to rescue overgrowth. Blood progenitor number is also sensitive to starvation and hypoxia in a TOR-dependent manner. Differences between *Tsc1/2* and *Pten* function become apparent at later stages. Loss of *Tsc1/2* autonomously increases p4EBP and decreases pAKT levels, expands the number of intermediate progenitors and limits terminal differentiation, except for a late induction of lamellocytes. By contrast, absence of PTEN increases p4EBP and pAKT levels and induces myeloproliferative expansion of plasmatocytes and crystal cells. This increased malignancy is associated with non-autonomous increases in p4EBP levels within peripheral differentiating hemocytes, culminating in their premature release into circulation and demonstrating potential non-autonomous effects of *Pten* dysfunction on malignancy. This study highlights mechanistic differences between TSC and PTEN on TOR function and demonstrates the multifaceted roles of a nutrient-sensing pathway in orchestrating proliferation and differentiation of myeloid-specific blood progenitors through regulation of ROS levels and the resulting myeloproliferative disorder when dysregulated.

**KEY WORDS: *Drosophila*, Lymph gland, Myeloid, TSC, PTEN, TOR**

## INTRODUCTION

The innate plasticity of hematopoietic progenitors is tightly regulated to continuously replenish blood cells under steady-state conditions and to supply cells that are immediately available in response to stress. Similar to vertebrates, hematopoiesis in *Drosophila* requires a population of multipotent progenitor cells (Mandal et al., 2007). These progenitors give rise exclusively to myeloid-like lineages through mechanisms that are conserved at the cellular and molecular levels (Evans and Banerjee, 2000; Evans et al., 2003; Martinez-Agosto et al., 2007).

Mature myeloid cell types derived from *Drosophila* progenitors include: macrophage-like plasmatocytes (PLs); crystal cells (CCs); and a specialized cell type, the lamellocyte, which is not normally present in the larva but can be induced to differentiate in response to specific immune challenges (Lanot et al., 2001; Sorrentino et al., 2002). One wave of hematopoiesis in *Drosophila* occurs in the larval lymph gland (LG) (Lebestky et al., 2000). In the LG, maturing hemocytes populate the peripheral cortical zone (CZ; Fig. 1A), and originate from a pool of multipotent progenitors that are compactly arranged in the medullary zone (MZ; Fig. 1A) and are genetically distinguishable by expression of the JAK/STAT receptor *domeless* (*dome*) (Jung et al., 2005). Additionally, a small population of intermediate progenitors is localized at the MZ/CZ boundary (Fig. 1A) (Sinenko et al., 2009; Krzemien et al., 2010). The posterior signaling center (PSC; Fig. 1A), a small group of cells at the posterior LG tip, functions as a hematopoietic niche by supplying pro-maintenance signals to progenitors (Krzemien et al., 2007; Mandal et al., 2007).

Proliferative and pro-differentiation cellular responses in *Drosophila* blood progenitors are mobilized in response to specific stimuli, such as increased reactive oxygen species (ROS) levels or parasitic wasp infection (Lanot et al., 2001; Sorrentino et al., 2002; Owusu-Ansah and Banerjee, 2009; Krzemien et al., 2010). This plasticity of the LG to adapt to stress scenarios and regulate its growth is reminiscent of the Target of rapamycin (TOR) signaling network. TOR is a conserved serine/threonine kinase that forms part of a multiprotein complex (TORC1) that coordinates cell growth in response to environmental signals such as energy status, nutrient availability and cellular stressors (Yang and Guan, 2007; Wang and Proud, 2009; Russell et al., 2011). Its growth-promoting function is largely effected by regulating protein translation downstream of two major effectors: S6 kinase (S6K) and the translational initiation factor 4E-binding protein (4E-BP; Fig. 1B) (Fingar et al., 2002; Holz et al., 2005; Ma and Blenis, 2009).

Regulation of TORC1 signaling through upstream mediators occurs largely at the level of the pathway inhibitor Tuberous sclerosis complex 1 and 2 (TSC1/2; Fig. 1B). TSC1/2 blocks TORC1 activation by inhibiting RHEB, the direct activator of TORC1 (Garami et al., 2003; Inoki et al., 2003; Tee et al., 2003). Perhaps the best-characterized modulator of TORC1 signaling is AKT, a kinase that is activated downstream of growth factor signaling in a phosphatidylinositol 3-kinase (PI3K)-dependent manner (Fig. 1B). Activated AKT phosphorylates TSC2 on multiple residues, which relieves RHEB inhibition and activates TORC1 (Inoki et al., 2002; Potter et al., 2002; Miron et al., 2003). PI3K-dependent activation of AKT is inhibited by the Phosphatase

[1]Molecular Biology Institute, University of California, Los Angeles, CA 90095, USA. [2]Department of Human Genetics, David Geffen School of Medicine, University of California, Los Angeles, CA 90095, USA.

*Author for correspondence (julianmartinez@mednet.ucla.edu)

**Accepted 16 July 2012**

and tensin homolog (PTEN; Fig. 1B) as well as by a negative-feedback loop downstream of TORC1 signaling (Harrington et al., 2004; Kockel et al., 2010), adding additional layers of regulation to AKT-mediated TORC1 activation.

In this study, we demonstrate the common effects of *Tsc2* and *Pten* loss on the regulation of early blood progenitor proliferation in a TORC1-, 4EBP- and ROS-dependent manner. We highlight differences in the expansion of intermediate progenitors and differentiated hemocytes that are unique to TSC and PTEN, as well as the roles of stress, feedback inhibition and AKT activity in TOR-dependent LG regulation.

## MATERIALS AND METHODS

### *Drosophila* stocks

All stocks were obtained from stock centers (VDRC, NIG, Bloomington) except: *UAS-Tsc1+2* [A. Gould (Tapon et al., 2001)]; *UAS-Pten^wt* and *Pten^C494* (A. Wodarz, Georg-August-Univ, Gottingen, Germany); *Tsc2^129* (T. Ip, University of Massachusetts, Medical Center, Worcester, MA, USA); *UAS-GTPx1* (U. Banerjee, University of California, Los Angeles, CA, USA); and *UAS-Akt^myr* [E. Hafen (Stocker et al., 2002)]; *w^1118* was used for controls. Gal4 lines used: *dome-gal4, UAS-2xEGFP*; and *dome-gal4; P{tubP-gal80[ts]}20* (U. Banerjee). *dome-gal4* crosses were performed at 29°C, except *dome>Tsc1+2*, *dome>Pten^wt* and *dome>Tor^DN* crosses which were grown at 18°C.

### Larval staging experiments

Staging of *dome>Tsc2*RNAi and *dome>Pten*RNAi was performed at 29°C, and the following time points after egg hatching (AEH) were used for larval stages: 30 hours AEH (early second instar, eL2); 36 hours AEH (late second instar, lL2); 42 and 48 hours AEH (early third instar, eL3); 54 hours AEH (mid third instar, mL3); 65 hours AEH (late third instar, lL3); and 72 hours AEH (wandering third instar, wL3).

### Clonal analysis

FLP-out clones in the LG were generated using *HHLT* (*hand-gal4, hml-gal4, UAS-2xEGFP, UAS-FLP, A5C-FRT-STOP-FRT-gal4*) as described (Evans et al., 2009). For lineage tracing of circulating hemocytes, H-TRACE (*hand-gal4, UAS-2xEGFP, UAS-FLP, A5C-FRT-STOP-FRT-gal4*) was used. Genotypes for MARCM FRT clones are as follows: *hs-flp FRT82B Tsc1^29 FRT82B Tub-mCD8-GFP* and *hs-flp FRT40A Pten^2L117 FRT40A Tub-nGFP*. Clones were induced by a 2-hour heat shock at 37°C within 2 hours AEH.

### Immunohistochemistry, BrdU labeling and ROS detection

Immunohistochemistry was performed as previously described (Jung et al., 2005). Antibodies used: mouse anti-PXN (1:400; L. Fessler, University of California, Los Angeles, CA, USA); rabbit anti-PPO (1:400; M. Kanost, Kansas State University, Manhattan, KS, USA); mouse anti-P1 and anti-L1 (both 1:20; I. Ando, Hungarian Academy of Sciences, Szeged, Hungary); rat anti-SHG (1:400; V. Hartenstein, University of California, Los Angeles, CA, USA); rabbit anti-p4EBP and anti-pAKT (1:300 and 1:40, respectively; Cell Signaling); mouse anti-LZ and anti-TSC2 (both 1:100; DSHB); rabbit anti-RHEB (1:200; Thermo Scientific); rabbit anti-PTEN (1:400; A. Wodarz); mouse anti-Histone (pan) (1:100; Millipore); and anti-phH3 (1:300; Millipore and AbCam). BrdU labeling was performed as previously described with a 45-minute BrdU pulse (Mondal et al., 2011). ROS detection was performed as previously described (Owusu-Ansah and Banerjee, 2009) using dihydroethidium.

### Rapamycin experiments

For early treatment, crosses were set up on 15-20 μM rapamycin food plates, and larvae were grown at 25°C until wL3. For later treatment, larvae were reared on normal food until eL3 and transferred to rapamycin food plates until wL3.

### Circulating hemocyte analysis

Circulating hemocytes from a single larva were isolated in 20 μl PBS and evenly dispersed on a 14 multi-well glass slide (Thermo Scientific), incubated for 30 minutes, and then fixed and immunostained as above. Relative quantification of circulating hemocytes is reported as the number of hemocytes per 0.25 $mm^2$ section of the glass well.

### Quantitative real-time PCR (Q-PCR)

Isolation of total RNA and reverse transcription were performed according to standard methods. Q-PCR was performed using an ABI 7900HT Q-PCR machine and SYBR Green (Qiagen). Relative quantification of transcript levels was calculated using the comparative $C_t$ method and normalized against *rp49* (*RpL32* – FlyBase). *Tsc2* and *rp49* primers were used as described (Amcheslavsky et al., 2011). *Pten* primers were: forward, 5′-GCCACAGAAAATGCAAAGCCA-3′; reverse, 5′-GCCGGAAAC-TGGTATTGATGGT-3′.

### Distribution of hemocyte and progenitor cell populations

Methodology to determine ratios of $dome^+$/$PXN^-$ prohemocyte, $dome^+$/$PXN^+$ intermediate progenitor and $dome^-$/$PXN^+$ differentiated hemocyte populations was adapted from Shim et al. (Shim et al., 2012). Two-way ANOVA analysis was used to evaluate significance between hemocyte population distributions among genotypes.

### Mitotic index and CC ratios

Mitotic index and ratio of CCs in the LG were measured as the total number of $phH3^+$ or $LZ^+$/$PPO^+$ cells divided by the total number of cells. The method for estimating total cell numbers in the LG was adapted from Krzemien et al. (Krzemien et al., 2010). The distribution of mitoses at mL3 was assessed by quantifying the number of $phH3^+$ cells in each population for all confocal sections as a ratio to total $phH3^+$ hemocytes. Statistical significance was evaluated with Student's *t*-test (mitotic index and CC ratios) and two-way ANOVA analysis (distribution of mitoses).

### Starvation and hypoxic stress

Acute starvation was induced by transferring (fed) eL3 larvae (48 hours AEH at 29°C) to agar plates containing PBS/1% sucrose for 24 hours; larvae were dissected at 72 hours AEH. For hypoxia experiments, larvae were reared in normoxia until lL2 (36 hours AEH at 29°C) and then transferred to a 5% $O_2$ hypoxia chamber until wL3.

## RESULTS

### TSC and PTEN regulate TORC1 signaling in *Drosophila* blood progenitors

A search for cell type-specific markers in the LG identified higher expression of RHEB and TSC2 in MZ progenitors (prohemocytes) than in CZ hemocytes at wL3 (Fig. 1C-D′). Similar expression was observed for the upstream regulator of TORC1 activity, PTEN (Fig. 1E,E′), as well as for phosphorylated (p) AKT (AKT1 – FlyBase) (Fig. 1F,F′), indicating that active PI3K-AKT signaling occurs in prohemocytes. Expression of p4EBP (THOR – FlyBase), a marker of active TOR kinase activity (Miron et al., 2003), was also higher in MZ prohemocytes (Fig. 1G,G′). We confirmed the central role for TSC in regulating TORC1 signaling during normal *Drosophila* hematopoiesis by examining p4EBP expression upon *Tsc1/2* loss-of-function (LOF). *Tsc1* and *Tsc2* (*gigas* – FlyBase) homozygous mutants die at early larval stages (Ito and Rubin, 1999). Interestingly, heterozygosity for mutations in *Tsc1* or *Tsc2* specifically increases p4EBP levels in $dome^+$ progenitors at wL3 (supplementary material Fig. S1A-C′), whereas heterozygosity for a *Pten* mutation increases p4EBP throughout the LG (supplementary material Fig. S1D,D′). A similar effect occurs upon progenitor-specific downregulation of *Tsc2* or *Pten* in the LG (supplementary material Fig. S1E-F′).

We next examined the phenotypic consequence of TORC1 hyperactivation, induced by downregulation of *Tsc1/2* or *Pten* function, on hemocyte progenitors. Growth of the LG occurs via extensive cell proliferation throughout larval development, from an initial group of ~30 progenitors per lobe in the late embryo to a

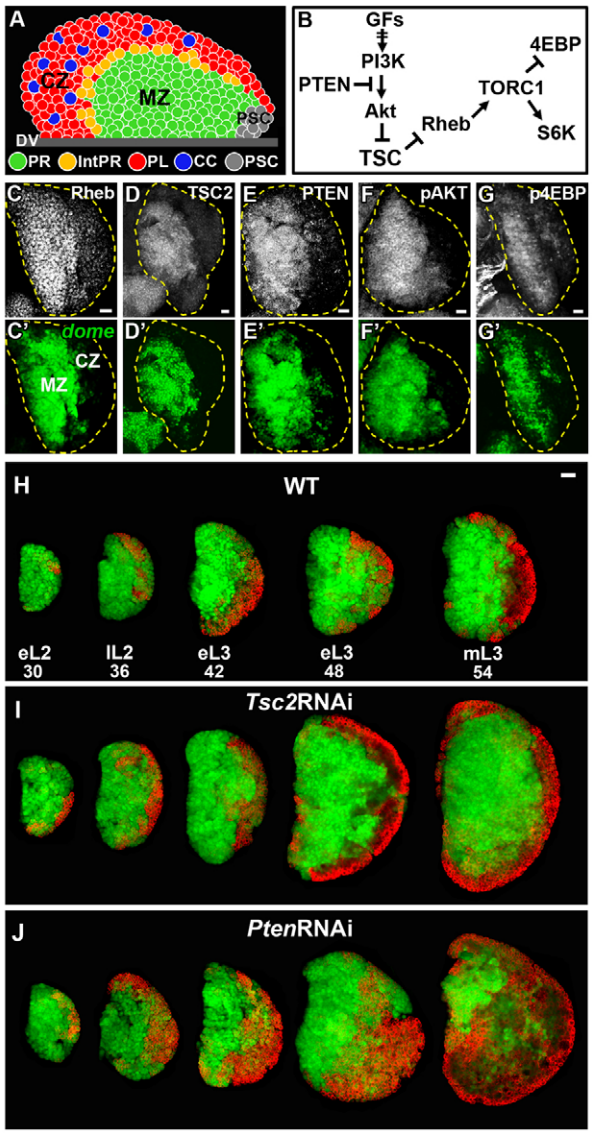


**Fig. 1. TORC1 signaling in *Drosophila* hemocyte progenitors regulates early LG growth.** (**A**) Diagram of a wL3 lymph gland (LG) primary lobe, highlighting undifferentiated progenitors (PRs) in the medullary zone (MZ), plasmatocytes (PLs) and crystal cells (CCs) in the cortical zone (CZ), intermediate progenitors (IntPrs) and the posterior signaling center (PSC). DV, dorsal vessel. (**B**) TOR signaling to its targets 4EBP and S6K is inhibited by TSC and PTEN. GFs, growth factors. (**C-G′**) TORC1 pathway components are expressed in MZ progenitors. All panels show wild-type (WT; *dome-gal4, UAS-2xEGFP*) wL3 LGs (outlined by dashed line). Expression of RHEB (C,C′), TSC2 (D,D′), PTEN (E,E′), pAKT (F,F′) and p4EBP (G,G′) is elevated in prohemocytes (green). (**H-J**) *dome-gal4, UAS-2xEGFP* (H) is used to express *UAS-Tsc2*RNAi (I) or *UAS-Pten*RNAi (J) in prohemocytes (green). The early differentiation marker PXN is in red. (H) Progression of WT growth from eL2 to mL3 instar stages. (I,J) *Tsc2* (I) and *Pten* (J) downregulation increases LG growth rate throughout development. *Pten* LOF increases differentiation by 36 hours AEH and throughout later stages. Scale bars: 20 μm.

mature LG consisting of ~5000 hemocytes (Krzemien et al., 2010). Onset of differentiation occurs during the second larval instar stage (L2), invariably at the periphery of the tissue (Fig. 1H). Early differentiating hemocytes express both the prohemocyte marker *dome* and the early differentiation marker Peroxidasin (PXN) at low levels (*dome*$^{+}$/PXN$^{+}$), and represent a population of intermediate progenitors. By contrast, fully differentiated hemocytes lose *dome*, upregulate PXN expression (*dome*$^{-}$/PXN$^{+}$), and proceed to express a marker of terminal differentiation: P1 (PLs), Prophenoloxidase (PPO; CCs) or L1 (lamellocytes). *Tsc2* or *Pten* downregulation in prohemocytes increases the rate of tissue growth during L2, eL3 and mL3 instar stages (Fig. 1I,J). In *Tsc2*-deficient LGs, differentiation onset and progression remain intact (compare Fig. 1H with 1I), and, accordingly, the proportion of *dome*$^{+}$/PXN$^{-}$ prohemocytes by mL3 (64%) is the same as in wild type (WT; 65%) (supplementary material Fig. S1G). By contrast, *Pten* deficiency expands differentiating hemocytes from lL2 to mL3 (Fig. 1J and supplementary material Fig. S1G), suggesting a specific role for PTEN in prohemocytes in regulating their transition to differentiation during development.

## TORC1 activity correlates with early proliferating progenitors

The accelerated rate of tissue growth that we observe upon *Tsc2* and *Pten* LOF suggested that they might regulate LG proliferation. We tested this hypothesis by comparing the populations of phospho-histone H3 (phH3)$^{+}$ cells in WT versus *Tsc2*- or *Pten*-deficient LGs, and observed an increased number of mitotically dividing cells upon *Tsc2* or *Pten* disruption throughout all stages (compare Fig. 2A,D,G with 2B,E,H and 2C,F,I). The percentage of phH3$^{+}$ cells in the developing LG (mitotic index) is highest during L2 and eL3 (Fig. 2J) (Krzemien et al., 2010). Importantly, we found that the mitotic index of *Tsc2*- or *Pten*-deficient LGs is significantly increased during this critical window of LG growth (Fig. 2J), accounting for the increased rate of tissue growth observed (Fig. 1H-J). Interestingly, high levels of cytoplasmic p4EBP (p4EBP$^{high}$) are expressed in a small population of scattered cells (Fig. 2A′,D′) in WT LGs during L2 and eL3, the majority of which colocalize with phH3 and represent mitotically dividing hemocytes (Fig. 2A″,D″). Downregulation of either *Tsc2* or *Pten* in progenitors increases the population of phH3$^{+}$/p4EBP$^{high}$ cells at these early stages (Fig. 2B″,E″ and 2C″,F″), suggesting that TORC1 activity promotes the early proliferation and expansion of progenitor pools. Expression of high p4EBP levels in phH3$^{+}$ cells during early larval development is specific for M phase, as overlap of p4EBP with the S-phase marker BrdU is not observed in any background (supplementary material Fig. S1H-M).

By mL3 the mitotic index drops significantly in WT, but more dramatically in *Tsc2*- or *Pten*-deficient backgrounds (Fig. 2J), emphasizing their role during the phases of highest proliferation in early LG development. Moreover, a higher proportion of mitoses in *Pten*-deficient LGs at mL3 occur within PXN$^{+}$ hemocytes as compared with WT or *Tsc2*-deficient LGs (supplementary material Fig. S1N), consistent with the increased differentiation observed at mL3 (Fig. 1J and supplementary material Fig. S1G). In addition, the population of p4EBP$^{high}$ cells at mL3 in *Tsc2*- and *Pten*-deficient LGs is much larger than that of phH3$^{+}$ cells, although some colocalization still occurs (Fig. 2H″,I″).

## Dynamic p4EBP expression downstream of *Pten* and *Tsc2* deficiencies at later third instar stages

The significant increase in p4EBP levels in *Tsc2*- or *Pten*-deficient LGs by mL3 (Fig. 2H″,I″) occurs during a stage when increased differentiation in the LG expands the early CZ. In both *Tsc2*- and *Pten*-deficient backgrounds at mL3, a pronounced accumulation of p4EBP occurs in differentiating cells that express low levels of

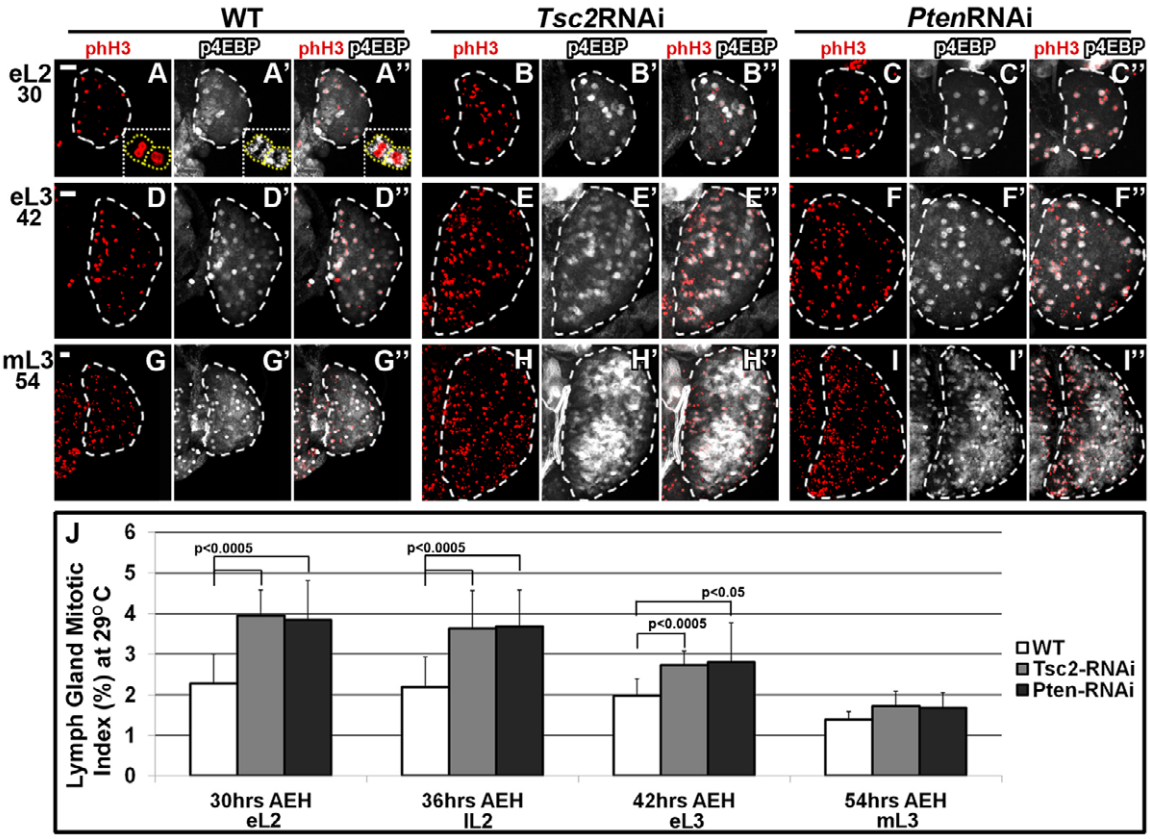


**Fig. 2. TORC1 activity in early proliferating prohemocytes.** (**A-A″**,**D-D″**,**G-G″**) p4EBP expression (white) in WT (*dome*>) overlaps with mitotically dividing cells (phH3, red). Inset (A-A″) demonstrates cytoplasmic p4EBP accumulation. (**B-C″**,**E-F″**,**H-I″**) Downregulation of *Tsc2* (*dome*>*Tsc2*RNAi) or *Pten* (*dome*>*Pten*RNAi) increases the number of proliferating cells and p4EBP$^{high}$ cells, which colocalize at early stages (B″,E″,C″,F″) but not at mL3 (H″,I″). (**J**) Quantification of LG mitotic index. *Tsc2* or *Pten* downregulation significantly increases LG mitotic index at early developmental stages. Data are mean ± s.d., *n*=12. Scale bar: 20 μm (for each row).

PXN along the early MZ/CZ boundary (Fig. 3A-F‴), marking a transition in high TORC1 activation from proliferating hemocytes to differentiating hemocytes at mL3. A subset of these p4EBP$^{high}$ cells express low levels of P1 (supplementary material Fig. S2A-C‴, arrows) but not the CC progenitor marker Lozenge$^{+}$ (LZ$^{+}$; supplementary material Fig. S2D-F‴), demonstrating that high p4EBP expression is specific for differentiating *dome*$^{+}$/PXN$^{+}$ or P1$^{low}$ PLs, and not for fully differentiated (*dome*$^{-}$) PLs at the LG periphery or CC progenitors. Lamellocytes are not observed at this stage.

At lL3 (Fig. 3G-I‴), the p4EPB patterns become markedly distinct between *Tsc2*- and *Pten*-deficient LGs (compare Fig. 3H″ with 3I″). High p4EBP expression extends medially in *Tsc2*-deficient LGs, overlapping largely with *dome*$^{+}$/PXN$^{+}$ cells, and is absent in the LG periphery (Fig. 3H-H‴). By contrast, high p4EBP expression extends peripherally in differentiating hemocytes in *Pten*-deficient LGs, including within buds of tissue that pinch off from the CZ, and is expressed at lower levels in MZ prohemocytes (Fig. 3I-I‴). By wL3, p4EBP$^{high}$ cells are observed in *dome*$^{+}$ hemocytes in both backgrounds, but continue to extend peripherally upon progenitor-specific *Pten* downregulation (supplementary material Fig. S1E-F′). Collectively, these data demonstrate non-autonomous activation of TORC1 activity upon *Pten*, but not *Tsc2*, downregulation in progenitors at late stages.

We further confirmed our findings from *Tsc1/2* and *Pten* deficiencies by performing mutant clonal analysis. Consistent with our findings from when *Tsc2* is downregulated in progenitors, high levels of p4EBP are autonomously upregulated in *Tsc1*$^{-/-}$ clones (Fig. 4B-B″). Although low levels of PXN are expressed in *Tsc1*$^{-/-}$ cells (Fig. 4B‴, gray), fully differentiated PXN$^{high}$ cells are found only at the very periphery of the LG (Fig. 4B‴, white), which are p4EBP negative. By contrast, accumulation of p4EBP in *Pten*$^{-/-}$ cells depends on clone location. Medially localized *Pten*$^{-/-}$ cells are p4EBP$^{low}$ and undifferentiated, similar to *Pten* downregulation in prohemocytes (Fig. 4D-D‴, yellow arrows; compare with Fig. 3I-I‴). Scattered p4EBP$^{high}$ expression is observed within a subset of more peripheral *Pten*$^{-/-}$ cells, as well as non-autonomously within WT PXN$^{high}$ cells (Fig. 4D-D‴, white arrows). Interestingly, the localization of large *Pten*$^{-/-}$ clones in the most peripheral LG regions was more likely associated with autonomous p4EBP upregulation (Fig. 4E,E′), differentiation, and 'pinching off' of LG tissue (Fig. 4F,F′), suggesting that the absence of *Pten* function might selectively affect differentiating hemocyte progenitors as opposed to the undifferentiated prohemocyte population. Furthermore, these findings substantiate the differences observed upon progenitor-specific downregulation of *Pten* and *Tsc*.

## *Tsc2* and *Pten* deficiencies expand distinct cell populations at wandering third instar

In addition to their divergent p4EBP patterns at late stages, striking differences are observed between *Tsc2*- and *Pten*-deficient LGs in the expansion of distinct cell lineages by wL3. Whereas WT LGs

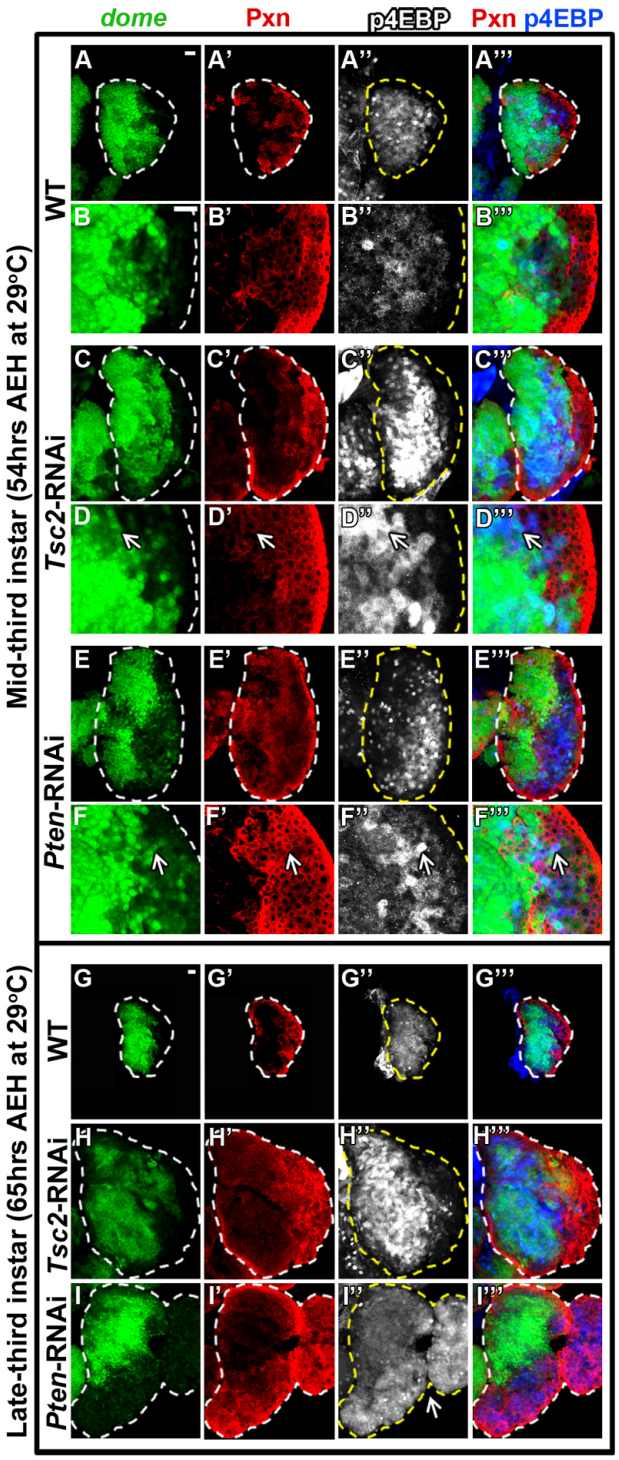


**Fig. 3. Dynamic p4EBP expression at mid and late third instar stages.** p4EBP expression is white in column 3 and blue in column 4. (**A-B‴**,**G-G‴**) In WT (*dome-gal4, UAS-2xEGFP*), p4EBP is expressed at low levels and in scattered p4EBP$^{high}$ cells. (**C-F‴**,**H-I‴**) Downregulation of *Tsc2* (*dome>Tsc2*RNAi) or *Pten* (*dome>Pten*RNAi) in progenitors expands a population of p4EBP$^{high}$ cells along the MZ/CZ boundary at mL3 (C-F‴). Arrows in D-D‴ and F-F‴ point to PXN$^{+}$/p4EBP$^{high}$ cells. By lL3, high p4EBP expression expands throughout medial regions upon *Tsc2* downregulation (H-H‴), but is highest upon *Pten* downregulation in differentiating cells at the LG periphery (I-I‴), including within buds of CZ tissue (arrow, I′). Scale bars: 20 μm; in A for A-A‴,C-C‴,E-E‴; in B for B-B‴,D-D‴,F-F‴; in G for G-I‴.

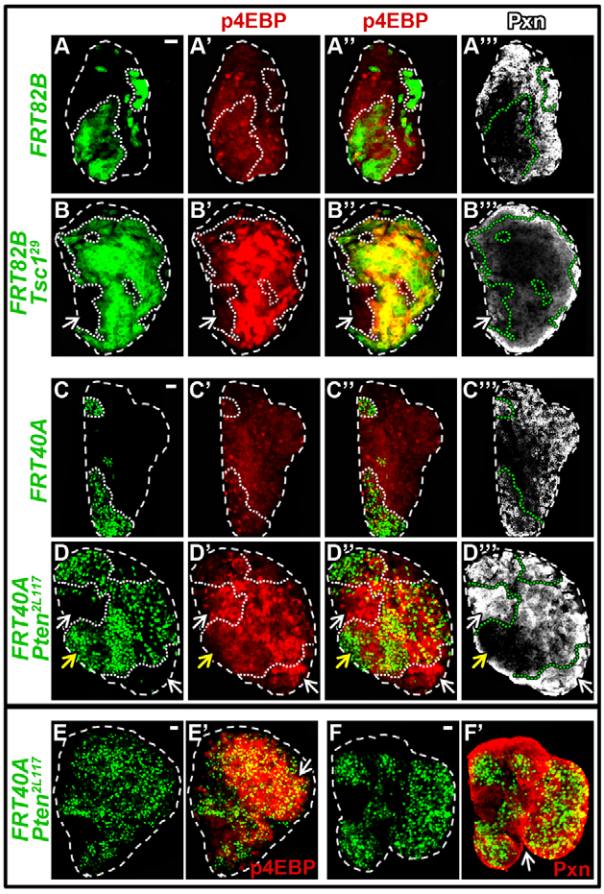


**Fig. 4. Mutant clonal analysis of *Tsc1* and *Pten* in the LG.** All panels show lL3. Clones are outlined by a white or green dotted line. (**A-B‴**) *Tsc1* MARCM clones. (A-A‴) WT MARCM clones (*hs-flp FRT82B Tub-mCD8-GFP*). (B-B‴) *Tsc1*$^{29}$ clones (*hs-flp FRT82B Tsc1*$^{29}$ *FRT82B Tub-mCD8-GFP*) express elevated p4EBP (red) in *Tsc1*$^{-/-}$ clones (green) relative to surrounding WT tissue (arrows). High PXN expression (white) is observed only at the tissue periphery, whereas *Tsc1*$^{-/-}$ cells express low PXN levels (gray, B‴). (**C-F′**) *Pten* MARCM clones. (C-C‴) WT MARCM clones (*hs-flp FRT40A Tub-nGFP*). (D-F′) *Pten*$^{2L117}$ clones (*hs-flp FRT40A Pten*$^{2L117}$ *FRT40A Tub-nGFP*) express high p4EBP (red) within scattered *Pten*$^{-/-}$ cells as well as in surrounding WT cells, which are also PXN$^{+}$ (white arrows in D-D‴). Medial *Pten*$^{-/-}$ cells are PXN negative and express low p4EBP levels (yellow arrows in D-D‴). *Pten*$^{-/-}$ clones located in peripheral LG regions are associated with high p4EBP (red) levels (arrow, E,E′) and pinching off of PXN$^{+}$ (red) tissue (arrow, F,F′). Scale bars: 20 μm.

have a small population of intermediate progenitors at the MZ/CZ boundary (5±2% of the LG; Fig. 5A-A″,P), as identified by co-expression of *dome* and PXN (Fig. 5A-A″, insets), *Tsc2* downregulation in the MZ induces severe LG overgrowth and dramatically expands the proportion of *dome*$^{+}$/PXN$^{+}$ intermediate progenitors (51±10%; $P$<0.0001; Fig. 5E-E″,P). This proportion of *dome*$^{+}$/PXN$^{+}$ cells at wL3 is much higher than that observed at mL3 (supplementary material Fig. S1G), demonstrating a late accumulation of intermediate progenitors upon *Tsc2* downregulation. By contrast, the population of fully differentiated hemocytes (*dome*$^{-}$/PXN$^{+}$) decreases relative to WT (23±4% versus 40±3%, respectively; $P$<0.0001; Fig. 5P). Terminally differentiated PLs and CCs are found only in a thin cortical layer around the LG

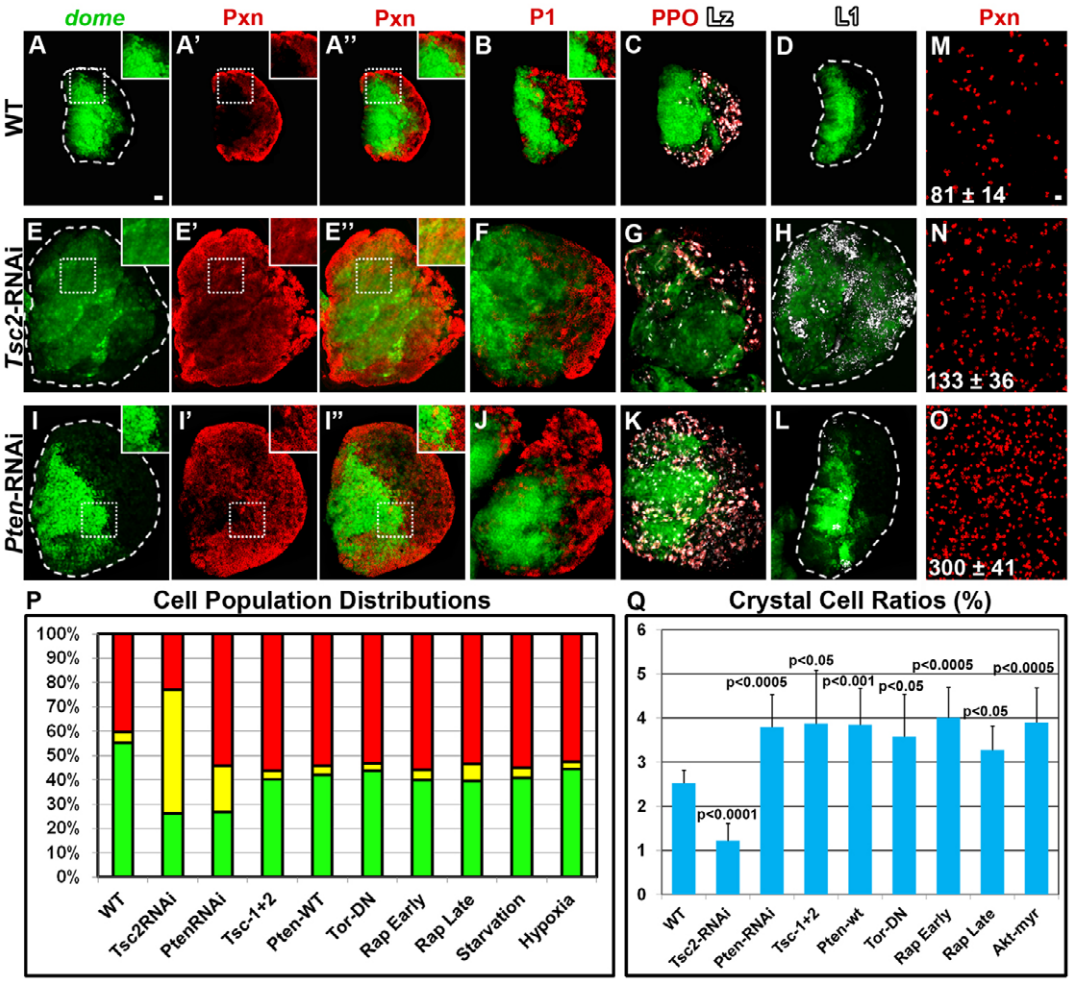


**Fig. 5. Effects of *Tsc2* and *Pten* deficiencies on differentiation.** All panels show wL3. (**A-D**) In WT (*dome-gal4, UAS-2xEGFP*), PXN (red) is expressed in differentiated hemocytes as well as in a small number of intermediate progenitors (*dome*$^{+}$/PXN$^{+}$) at the MZ/CZ boundary (insets, A-A″). (**B**) P1 (red) labels terminally differentiated PLs but not intermediate progenitors (inset). (**C**) PPO (red) marks fully differentiated CCs. LZ (white) marks both fully differentiated CCs (LZ$^{+}$/PPO$^{+}$) and CC progenitors (LZ$^{+}$/*dome*$^{+}$). (**D**) L1 marks lamellocytes, which are not present in WT. (**E-H**) *Tsc2* downregulation (*dome>Tsc2*RNAi) increases LG size and expands the population of intermediate progenitors (E-E″), decreases PLs (F) and CCs (G), and increases lamellocyte number (H). (**I-L**) *Pten* downregulation (*dome>Pten*RNAi) increases LG size and numbers of intermediate progenitors (I′,I″), PLs (J) and CCs (K) and of rare lamellocytes (L). (**M-O**) *Pten* downregulation (*dome>Pten*RNAi) (O) increases the relative number of circulating PXN$^{+}$ hemocytes compared with WT ($P$<0.0001; M) or *Tsc2* downregulation ($P$<0.0001; N). Data are mean ± s.d., $n$=8. (**P**) Distribution of *dome*$^{+}$/PXN$^{-}$ prohemocytes (green), *dome*$^{+}$/PXN$^{+}$ intermediate progenitors (yellow) and *dome*$^{-}$/PXN$^{+}$ differentiated hemocytes (red). Data are mean ($n$=12), and two-way ANOVA revealed significant changes ($P$<0.0001) in the distribution of hemocyte populations in all conditions compared with WT. (**Q**) Ratio of CCs to total LG cells (percentage). Data are mean ± s.d., $n$=10. Scale bars: 20 μm, except for 1.2× magnification for H,K.

periphery (Fig. 5F,G), and the ratio of CCs to total LG cells is significantly reduced compared with WT (Fig. 5Q). By contrast, lamellocytes, which are not normally present in a healthy larva (Fig. 5D), are dispersed throughout the LG (Fig. 5H). LG-specific clonal downregulation of *Tsc2* also induces overgrowth (supplementary material Fig. S3D-F), expands the population of PXN$^{+}$ hemocytes (supplementary material Fig. S3D′,D″) and induces lamellocytes (supplementary material Fig. S3F), demonstrating the LG-specific effects of *Tsc2* deficiency.

By contrast, *Pten* deficiency expands the populations of *dome*$^{+}$/PXN$^{+}$ intermediate progenitors (19±9%, compared with 5±2% in WT; $P$<0.0005; Fig. 5P), *dome*$^{-}$/PXN$^{+}$ cells (54±8%, compared with 40±3% in WT; $P$<0.0005; Fig, 5I-I″,P) and fully differentiated PLs (Fig. 5J) at the cost of the MZ. Unlike *Tsc2* downregulation, the ratio of CCs to total LG cells is significantly increased in the LG upon progenitor-specific *Pten* downregulation (Fig. 5K,Q), and lamellocytes are rarely observed (Fig. 5L). Increased lamellocyte differentiation upon *Tsc1/2* versus *Pten* LOF was also demonstrated by LG-specific clonal downregulation (supplementary material Fig. S3F,I) and mutant clonal analysis (supplementary material Fig. S3M-P). *Pten* downregulation also increases the number of circulating hemocytes compared with WT or *Tsc2* deficiency (compare Fig. 5O with 5M,N), suggesting premature dissemination of LG hemocytes upon *Pten* disruption, which do not normally enter circulation until the onset of metamorphosis when the LG disintegrates (Grigorian et al., 2011). Lineage-tracing analysis demonstrated the LG origin of the increased circulating hemocytes upon LG-specific *Pten* downregulation (supplementary material Fig. S3J-L). These phenotypic differences in *Tsc2*- and *Pten*-deficient LGs are not the

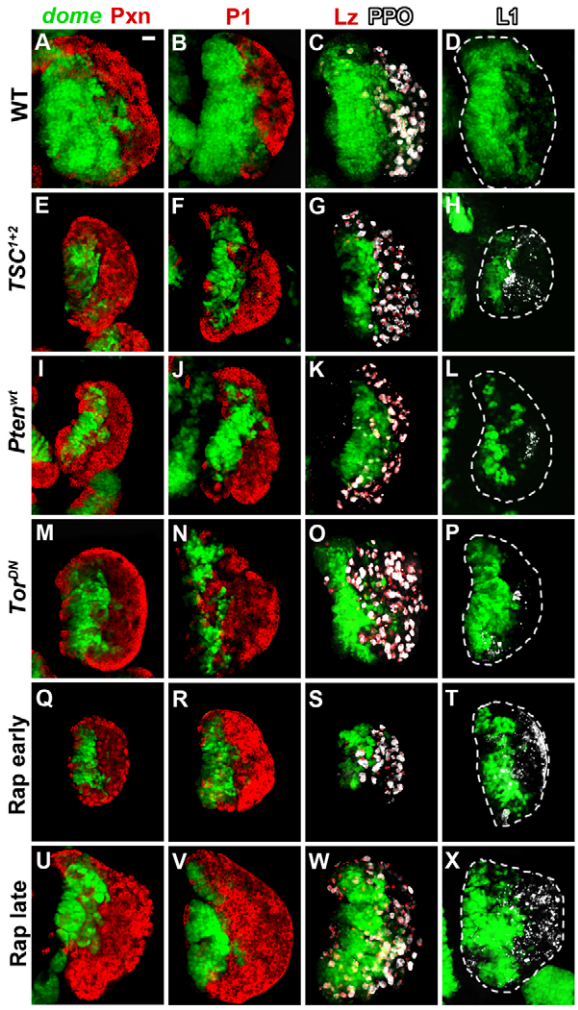


**Fig. 6. Inhibition of TORC1 signaling reduces progenitor pools.** All panels show wL3. *dome-Gal4, UAS-2xEGFP* (A-D) is used to express *UAS-Tsc*$^{1+2}$ (E-H), *UAS-Pten*$^{wt}$ (I-L) and *UAS-Tor*$^{DN}$ (M-P) in prohemocytes. (**A-D**) WT. The populations of PXN$^{+}$ hemocytes (A), PLs (P1, B), CCs (LZ$^{+}$/PPO$^{+}$, C) and lamellocytes (L1, D) are marked. (**E-T**) Overexpression of *Tsc*$^{1+2}$ (E-H), *Pten*$^{wt}$ (I-L) and *Tor*$^{DN}$ (M-P) or rapamycin treatment throughout larval development (Q-T) all decrease overall LG size (compare with A-D) and increase differentiation. (**U-X**) Rapamycin treatment only at late stages (eL3-wL3) does not affect LG size, but does increase differentiated hemocytes. Scale bar: 20 μm.

result of non-autonomous changes in PSC size (data not shown) or differences in knockdown efficiencies for their respective RNAi constructs (71% and 76% knockdown for *Tsc2*RNAi and *Pten*RNAi, respectively; supplementary material Fig. S3Q).

The premature dissemination of *Pten*-deficient LGs (Fig. 3I‴, Fig. 4F′ and supplementary material Fig. S3L) and scattering of *Pten* mutant cells within the LG (Fig. 4D) suggested that changes in cell adhesion might be associated with the greater malignancy of *Pten* versus *Tsc1/2* deficiency. High levels of Shotgun (SHG, DE-cadherin) expression are retained in *Tsc1*$^{-/-}$ clones, which express low levels of PXN (gray) and are not fully differentiated (PXN$^{high}$, white) (supplementary material Fig. S4B-B‴). Similarly, medially localized *Pten*$^{-/-}$ cells, which are undifferentiated, retain high SHG levels (supplementary material Fig. S4D-D‴, arrows). By contrast, scattered *Pten*$^{-/-}$ cells are PXN$^{high}$ and downregulate SHG expression (supplementary material Fig. S4D-D‴). Although the differentiation status of these scattered *Pten*$^{-/-}$ cells may account for the downregulation of SHG, we cannot rule out the possibility that decreased adhesion has a causative role in the increased differentiation and dissemination of *Pten*-deficient LGs.

## Inhibition of TORC1 signaling reduces progenitor pools and impairs early, but not late, LG growth

We next examined the phenotypic consequence of *Tsc1/2* and *Pten* overexpression on prohemocytes. Inhibition of TORC1 signaling by overexpression of *Tsc*$^{1+2}$ and *Pten*$^{wt}$ in progenitors reduces overall LG size at wL3 and significantly increases the proportion of PXN$^{+}$ hemocytes (Fig. 6A,E,I and Fig. 5P). Terminally differentiated hemocyte lineages are also expanded (Fig. 6F-H,J-L) and the ratio of CCs to total LG cells is significantly increased (Fig. 5Q). LG-specific clonal expression of *Tsc*$^{1+2}$ and *Pten*$^{wt}$ also decreases total LG size and increases differentiation throughout the tissue (supplementary material Fig. S5A-C). At L2, LGs in which prohemocytes overexpress *Tsc*$^{1+2}$ or *Pten*$^{wt}$ are already markedly smaller than controls (supplementary material Fig. S5D-F), which can be attributed to reduced progenitor proliferation at this stage (supplementary material Fig. S5G).

The decreased LG size and increased differentiation that we observe upon *Tsc*$^{1+2}$ or *Pten*$^{wt}$ overexpression is phenocopied by overexpression of a dominant-negative *Tor* allele in progenitors and through systemic treatment with the TORC1 inhibitor rapamycin (Fig. 6M-T). Both conditions increase the proportion of *dome*$^{-}$/PXN$^{+}$ hemocytes in the LG as well as the ratio of CCs to total LG cells (Fig. 5P,Q). Delaying treatment with rapamycin until later stages is sufficient to increase hemocyte differentiation as well (Fig. 6U-X and Fig. 5P,Q), but does not significantly affect further LG growth. A similar effect occurs upon conditionally overexpressing *Tsc*$^{1+2}$ in prohemocytes only after larvae reach later stages (supplementary material Fig. S5H-I″). These results highlight the early role of TORC1 signaling in regulating prohemocyte proliferation and a later role in regulating differentiation.

## *Tsc2* and *Pten* phenotypes are sensitive to stress and depend on TORC1, 4EBP and pAKT

That a nutrient-sensing signaling pathway regulates progenitor number during normal *Drosophila* hematopoiesis raises the intriguing possibility that nutritional/environmental stress signals might utilize the same developmental hematopoietic signaling pathway to regulate progenitor adaptations to stress. The response of blood progenitors to stress conditions is evident upon rearing WT larvae under acute starvation and hypoxia, both of which increase the size of the CZ at the expense of MZ progenitors (Fig. 7A-A″ and Fig. 5P) and phenocopy conditions of reduced TORC1 signaling induced by overexpression of *Tsc*$^{1+2}$ and *Pten*$^{wt}$ (Fig. 5P). Furthermore, the LG overgrowth characteristic of *Tsc2*- and *Pten*-deficient LGs is attenuated by these stressors (Fig. 7B-B″,C-C″), suggesting that the effects of starvation and hypoxia on hemocyte progenitors might be mediated by reducing TORC1 signaling.

We confirmed the TORC1 dependence of *Tsc2* or *Pten* deficiency-induced LG overgrowth by treating larvae with rapamycin throughout development, which was sufficient to rescue the phenotype in both backgrounds (Fig. 7B‴,C‴). The tight correlation of p4EBP expression with mitotically dividing cells during early LG development suggested that 4EBP might

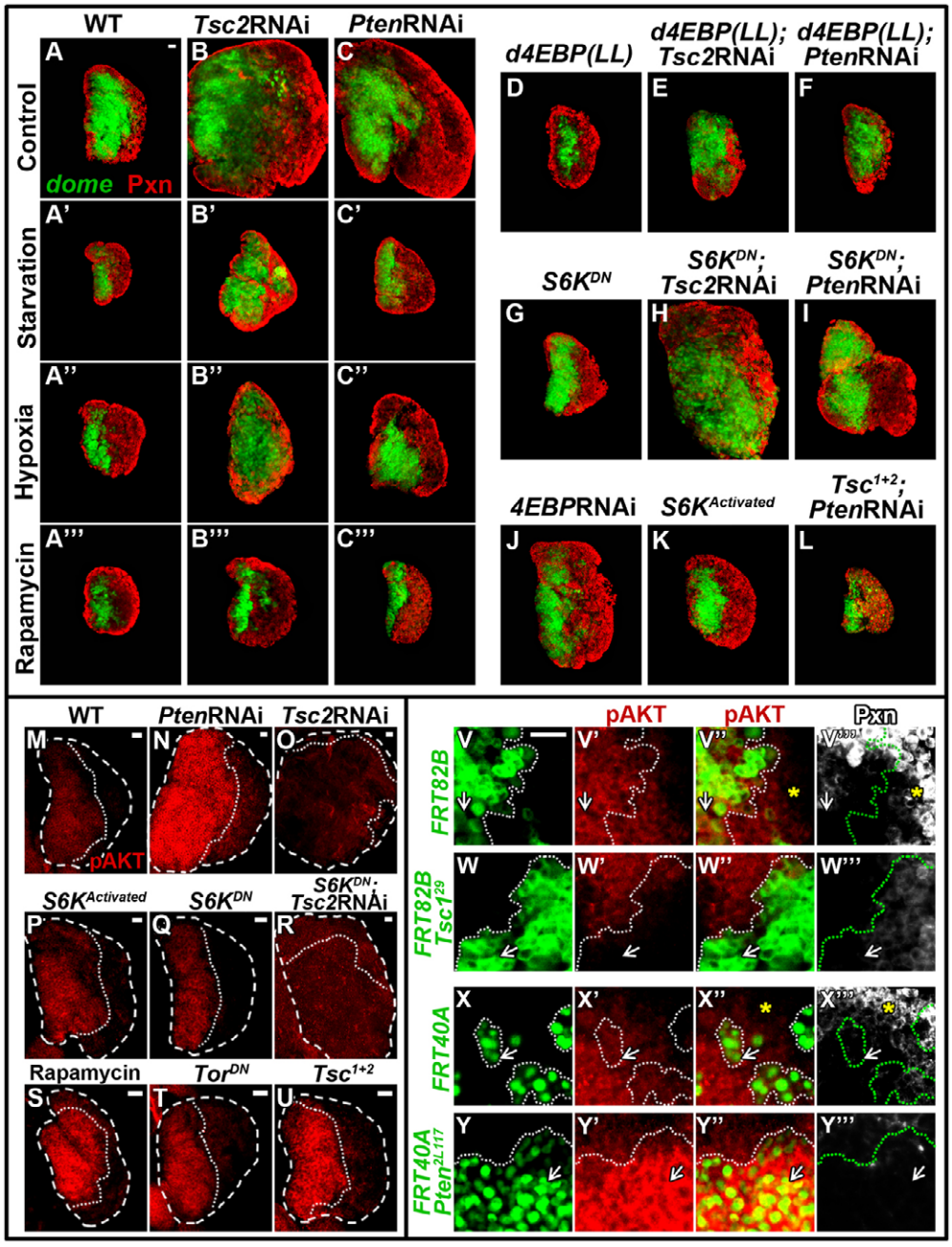


**Fig. 7. Dependence of *Tsc2* and *Pten* phenotypes on TORC1 and 4EBP but not S6K.** All panels show wL3. In A-U, *dome-gal4, UAS-2xEGFP* is used to drive expression of the specified genetic constructs (green channel is omitted in M-U, but *dome*$^{+}$ progenitors are outlined by dotted lines). PXN is in red in A-L and pAKT is in red in M-Y‴. (**A-A‴**) WT LGs (*dome*>). Starvation (A′), hypoxia (A″) or rapamycin treatment (A‴) all increase PXN$^{+}$ hemocytes (red) at the expense of MZ prohemocytes (green) compared with controls (fed/normoxic, A). (**B-C‴**) Overgrowth associated with *Tsc2* and *Pten* downregulation (B,C) is attenuated in conditions of starvation (B′,C′), hypoxia (B″,C″) and rapamycin treatment (B‴,C‴). (**D-F**) Overexpression of *d4EBP(LL)* decreases LG size (D) and is sufficient to attenuate LG overgrowth in *Tsc2*-deficient (E) or *Pten*-deficient (F) LGs (compare with B,C). (**G-I**) Reducing S6K function (*dome>S6k*$^{DN}$) does not affect LG size and differentiation (G), and does not rescue LG overgrowth in *Tsc2*-deficient (H) or *Pten*-deficient (I) LGs. (**J**,**K**) Downregulation of *4EBP* (J) increases LG size to a greater extent than activation of S6K (K). (**L**) Overexpression of *Tsc*$^{1+2}$ upon *Pten* downregulation rescues LG overgrowth but does not rescue the increased differentiation observed upon *Pten* downregulation alone (compare with C). (**M**) WT LG. Expression of pAKT is highest medially, within *dome*$^{+}$ progenitors. (**N**,**O**) *Pten* downregulation increases pAKT levels in progenitors (N), whereas *Tsc2* deficiency reduces pAKT expression (O). (**P**,**Q**) Activating (*dome>S6k*$^{Activated}$, P) or reducing (*dome>S6k*$^{DN}$, Q) S6K function does not affect pAKT expression. (**R**) Downregulation of *S6k* activity upon *Tsc2* downregulation does not increase pAKT levels compared with conditions of *Tsc2* downregulation alone (compare with O). (**S-U**) Reducing TORC1 signaling via systemic rapamycin treatment (S) or overexpression of *Tor*$^{DN}$ (T) or *Tsc*$^{1+2}$ (U) in prohemocytes increases pAKT expression. (**V-Y‴**) MARCM clones for WT [*hs-flp FRT82B Tub-mCD8-GFP* (V-V‴) and *hs-flp FRT40A Tub-nGFP* (X-X‴)], *Tsc1*$^{29}$ (*hs-flp FRT82B Tsc1*$^{29}$ *FRT82B Tub-mCD8-GFP*, W-W‴) and *Pten*$^{2L117}$ (*hs-flp FRT40A Pten*$^{2L117}$ *FRT40A Tub-nGFP*, Y-Y‴)]. In WT, pAKT expression is highest in PXN-negative cells (arrows, V-V‴ and X-X‴) and gradually decreases in PXN$^{+}$ cells (asterisk, V″,V‴ and X″,X‴). *Tsc1*$^{-/-}$ clones demonstrate reduced pAKT expression in progenitors (PXN-negative cells; arrows, W-W‴). *Pten*$^{-/-}$ clones in medial LG regions demonstrate autonomous increases in pAKT expression (PXN-negative cells; arrows, Y-Y‴). Scale bars: 20 μm; A for A-L; in V for V-Y‴.

itself be regulating the proliferation of blood progenitors. Phosphorylation of 4EBP by active TORC1 relieves translation initiation factor 4E (eIF-4E) from inhibitory 4EBP binding and promotes growth (Gingras et al., 2001). Expression of a mutant form of *Drosophila* 4EBP [*d4EBP(LL)*] that binds more tightly to eIF-4E decreases LG size and increases differentiation, similar to rapamycin treatment (compare Fig. 7D with 7A,A‴). Overexpression of *d4EBP(LL)* upon *Tsc2* or *Pten* downregulation in progenitors is sufficient to block LG overgrowth (Fig. 7E,F), confirming a role for 4EBP downstream of TSC and PTEN in hemocyte progenitor proliferation. Unexpectedly, overexpression of $S6k^{DN}$ in prohemocytes is not sufficient to significantly alter LG size and differentiation (Fig. 7G), or to rescue overgrowth of *Tsc2*- and *Pten*-deficient LGs (Fig. 7H,I). The more prominent role for 4EBP as compared with S6K in the LG is also demonstrated in that downregulation of *4EBP* in prohemocytes increases LG size compared with controls (compare Fig. 7J with 7A), whereas overexpression of

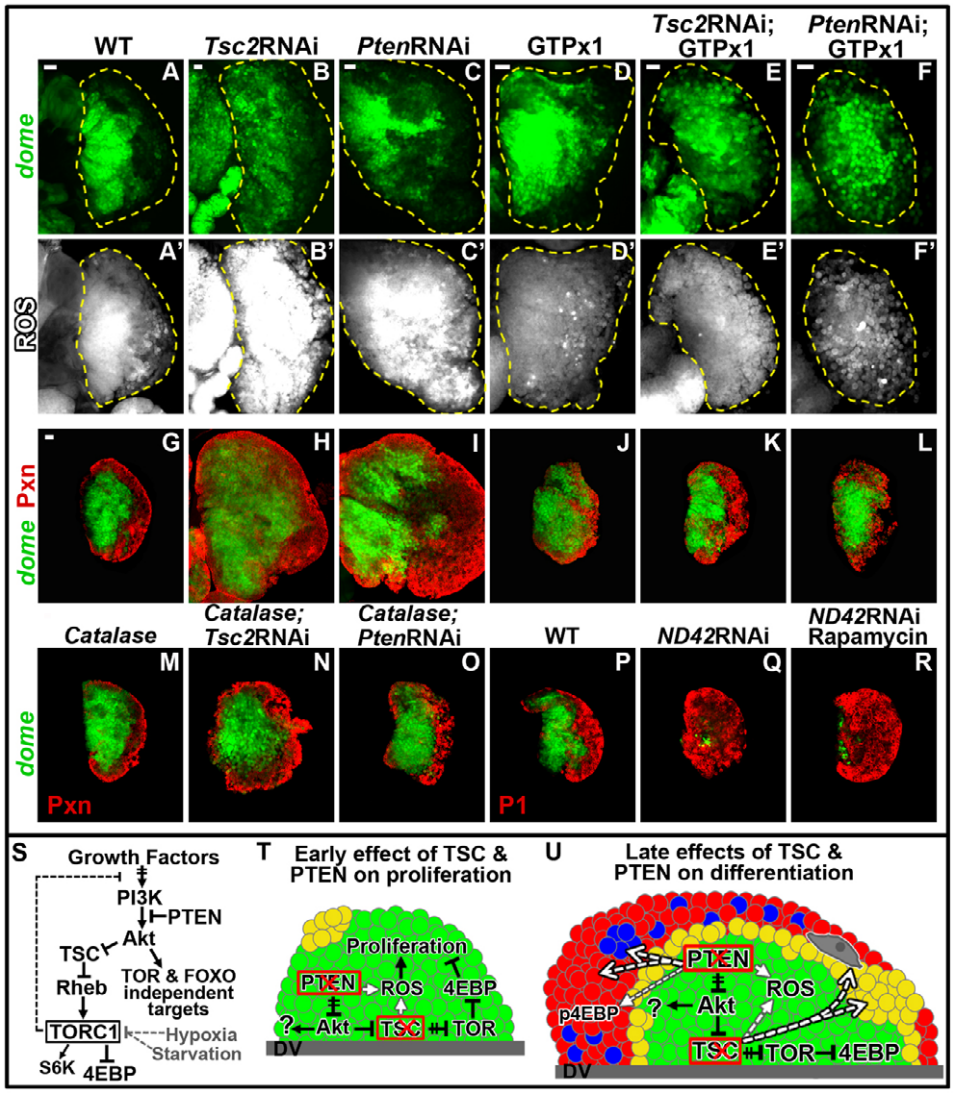


**Fig. 8. ROS-dependent effects of TSC and PTEN in prohemocytes.** All panels show wL3. *dome-gal4, UAS-2xEGFP* (green) drives expression of each genetic construct in prohemocytes. ROS levels are in white (A′-F′). PXN (G-O) or P1 (P-R) are in red. (**A**,**A′**) WT. ROS levels are highest in *dome*$^{+}$ prohemocytes. (**B-C′**) Downregulation of *Tsc2* (B,B′) or *Pten* (C,C′) increases ROS levels. (**D**,**D′**) Overexpression of the ROS scavenger GTPx1 reduces ROS levels. (**E-F′**) GTPx1 expression reduces ROS levels in *Tsc2*-deficient (E,E′) and *Pten*-deficient (F,F′) LGs. (**G-O**) Overexpression of the ROS scavengers GTPx1 (J) or catalase (M) upon *Tsc2* or *Pten* downregulation rescues their overgrowth (compare K,L and N,O with H,I). (**P**) WT LG. (**Q**) Downregulation of *ND42* increases PL differentiation and reduces the progenitor population (green) while LG size is unaffected. (**R**) Systemic rapamycin treatment of ND42-deficient LGs does not reverse the increase in differentiation. (**S**) TORC1 signaling to 4EBP (and S6K) is inhibited by TSC and PTEN. The presence of a TORC1-dependent negative-feedback loop in the LG regulates AKT activity upon TORC1 activation (crosshatched line). *Pten* disruption hyperactivates AKT, which can activate TORC1 signaling as well as TOR- and FOXO-independent effectors. Conditions of hypoxia and starvation are able to reduce TORC1 signaling downstream of PTEN and TSC. (**T**) Disruption of *Tsc2* and *Pten* in hemocyte progenitors (green) increase proliferation in a TOR-, 4EBP- and ROS-dependent manner at early stages. (**U**) At late LG stages, *Tsc1/2* and *Pten* deficiencies affect distinct hemocyte lineages. *Tsc1/2* disruption autonomously increases p4EBP and ROS levels and expands intermediate progenitors (yellow) and lamellocytes (gray). *Pten* disruption autonomously increases AKT activation and ROS levels, non-autonomously induces p4EBP expression and expands fully differentiated PLs (red) and CCs (blue). White arrows with gray outlines represent increases in specified marker expression; white arrows with black outlines represent increases in specified cell lineages. DV, dorsal vessel. Scale bars: 20 μm; in G for G-R.

*S6k*$^{Activated}$ does not (Fig. 7K). Epistasis of *Pten* and *Tsc1/2* was also examined, and, similar to rapamycin treatment, *Tsc*$^{1+2}$ overexpression is sufficient to block overgrowth of *Pten*-deficient LGs, although substantial differentiation still occurs (Fig. 7L). These data suggest that, although a common TOR-mediated signaling network regulates progenitor proliferation downstream of TSC and PTEN, TSC/TOR-independent effectors might contribute to the increased differentiation and myeloproliferative effects observed upon *Pten* deficiency.

One candidate effector molecule that may be differentially regulated upon *Tsc2* and *Pten* downregulation is AKT. Whereas *Pten* loss leads to constitutive activation of AKT, hyperactive TORC1 signaling is known to trigger a negative-feedback loop that attenuates PI3K-AKT signaling (Harrington et al., 2004; Kockel et al., 2010). *Pten* downregulation in prohemocytes increases pAKT levels in the LG (Fig. 7N), whereas pAKT expression is nearly absent in *Tsc2*-deficient LGs (Fig. 7O). Although this feedback inhibition downstream of TORC1 signaling could be S6K mediated (Harrington et al., 2004), we found no evidence of S6K-dependent feedback in *Drosophila* prohemocytes (Fig. 7P-R). By contrast, reducing TORC1 signaling in prohemocytes via rapamycin treatment (Fig. 7S), *Tor*$^{DN}$ overexpression (Fig. 7T), or *Tsc*$^{1+2}$ overexpression (Fig. 7U) did increase pAKT levels. Our data thus describe a TORC1-dependent, S6K-independent negative feedback that attenuates signaling to AKT in the LG.

Disparate pAKT expression among *Tsc2*- and *Pten*-deficient LGs raises the possibility that AKT might be a functionally relevant target downstream of PTEN but not TSC signaling, which might account for some of the observed phenotypic differences in these backgrounds. We confirmed differential regulation of pAKT upon *Tsc1/2* and *Pten* LOF through MARCM clonal analysis (Fig. 7V-Y‴), which demonstrates cell-autonomous increases in pAKT expression in medial *Pten*$^{-/-}$ cells, but absence of pAKT in *Tsc1*$^{-/-}$ cells. Although constitutive activation of AKT in prohemocytes does not induce hypertrophy, unlike in *Pten*-deficient LGs, we often observed an increase in PXN$^{+}$ cells, with occasional fragments of differentiated tissue ‘pinching’ off from the LG, similar to the effects of *Pten* loss (compare supplementary material Fig. S6C with S6B). Additionally, the ratio of CCs to total LG cells is significantly increased upon AKT activation (Fig. 5Q), whereas lamellocyte numbers are not altered (data not shown), further demonstrating the similarity of AKT-dependent phenotypes to *Pten* but not *Tsc1/2* loss. Perhaps the best-described targets of AKT are the Forkhead box O (FoxO) family of transcription factors, which are inhibited by activated AKT (Castellino and Durden, 2007). Downregulation of *foxo* in prohemocytes does not phenocopy *Pten* silencing or AKT activation (compare supplementary material Fig. S6D with S6B,C), and overexpression of *foxo* is not sufficient to rescue the increased differentiation or overgrowth of *Pten*-deficient LGs (supplementary material Fig. S6E,F). Although a common TORC1- and 4EBP-dependent signaling pathway mediates the early proliferative effects downstream of *Tsc2* and *Pten* deficiencies, the additive effects of activating both AKT and TORC1 signaling upon *Pten* disruption may account for the increased differentiation and myeloproliferation observed.

### ROS dependence of *Tsc2* and *Pten* phenotypes

Analysis of MZ markers that are affected upon progenitor-specific *Tsc2* or *Pten* disruption identified significant changes in ROS in these backgrounds. WT prohemocytes maintain elevated ROS levels at wL3 compared with differentiated hemocytes (Fig. 8A,A′) (Owusu-Ansah and Banerjee, 2009), and downregulation of *Tsc2* or *Pten* in progenitors increases ROS levels (Fig. 8B-C′). These levels are reduced upon overexpression of the ROS scavenger protein glutathione peroxidase-like 1 (GTPx1) in prohemocytes (Fig. 8E-F′). Scavenging ROS in *Pten*- and *Tsc2*-deficient LGs with GTPx1 (Fig. 8K,L) or catalase (Fig. 8N,O) is sufficient to rescue their overgrowth.

Downregulation of complex I proteins of the mitochondrial electron transport chain in prohemocytes, such as ND75 and ND42, has been previously shown to trigger precocious differentiation into mature hemocyte lineages (Owusu-Ansah and Banerjee, 2009). We examined whether elevated ROS is sufficient to induce the phenotypes associated with *Tsc2* and *Pten* deficiencies. Although downregulation of *ND42* in prohemocytes increases differentiation, LG size is unaffected (Fig. 8P,Q). Further, treating *ND42*-deficient larvae with rapamycin to suppress TORC1 signaling did not rescue the increased differentiation (Fig. 8R). These data demonstrate that the proliferative effects observed upon *Tsc2* and *Pten* disruption are ROS dependent, but differ in their phenotypic consequences and mechanistic basis from other conditions that may increase ROS in the LG (Owusu-Ansah and Banerjee, 2009).

## DISCUSSION

### TORC1 signaling regulates hemocyte progenitor proliferation

Our data demonstrate a crucial role of TORC1 signaling in regulating the proliferation of *Drosophila* hemocyte progenitors at early developmental stages, when rapid growth of the LG occurs. The specific accumulation of p4EBP in phH3$^{+}$ cells at early stages highlights the central function of TORC1 signaling in actively dividing hemocyte progenitors. These data complement recent findings in *Drosophila* ovarian germline stem cells (GSCs) in which p4EBP levels were specifically elevated in M phase (LaFever et al., 2010). However, in contrast to *Drosophila* GSCs, in which 4EBP does not mediate *Tor*-associated phenotypes (LaFever et al., 2010), our data demonstrate a central role for 4EBP in regulating hemocyte progenitor proliferation downstream of *Tsc* and *Pten* disruption (Fig. 8S,T). The sufficiency of scavenging ROS in *Pten*- and *Tsc2*-deficient LGs to rescue associated LG overgrowth also highlights the role of ROS in mediating hemocyte proliferation upon TORC1 hyperactivation (Fig. 8T). A limited number of studies in vertebrate hematopoietic stem cells (HSCs) deficient for *Tsc1* and *Pten* consistently demonstrate their initial expansion due to aberrant cell cycling, but eventual exhaustion caused by reduced self-renewal capacity (Yilmaz et al., 2006; Zhang et al., 2006; Chen et al., 2008). Our findings suggest that 4EBP-mediated TORC1 activity might be particularly relevant in hematopoietic progenitors, warranting its further investigation in vertebrates.

### Differential effects of *Tsc1/2* and *Pten* function on blood progenitors

Our findings demonstrate phenotypic differences upon *Tsc1/2* and *Pten* manipulation in blood progenitors. Mutant *Tsc1* clones autonomously express high levels of p4EBP and are associated with low PXN expression. Progenitor-specific downregulation of *Tsc2* does not alter differentiation onset and progression, but by late L3 stages the population of p4EBP$^{high}$ *dome*$^{+}$/PXN$^{+}$ intermediate progenitors dramatically expands, and retention of this pool of progenitors restricts the populations of fully differentiated PLs and CCs while still allowing large numbers of lamellocytes to differentiate (Fig. 8U). By contrast, *Pten* silencing promotes an

early increase in differentiation that proceeds to expand terminally differentiated PLs and CCs and also leads to premature release of hemocytes from the LG (Fig. 8U). Interestingly, the increased malignancy induced by *Pten* disruption in progenitors is associated with non-autonomous increases in p4EBP levels within peripheral differentiating hemocytes and 'buds' of CZ tissue (Fig. 8U, Fig. 3I″, Fig. 4D″ and supplementary material Fig. S1F). Further studies are needed to clarify whether non-autonomous TORC1 activation induced by *Pten* disruption is common to other cell types and might contribute to the greater malignancy potential associated with *PTEN* mutations as compared with *TSC* mutations in human disease (Manning et al., 2005).

In contrast to the non-autonomous effects of *Pten* LOF on p4EBP accumulation, *Pten* loss autonomously increases AKT activation. Further, the phenotypic similarities between AKT activation and *Pten* loss in progenitors suggests that the additive effects of activating both AKT and TORC1 signaling in *Pten*-deficient hemocytes might contribute to the more dramatic effects on terminal differentiation and premature release of LG hemocytes into circulation. Previous studies in vertebrates have shown that *Pten* loss (Yilmaz et al., 2006; Zhang et al., 2006) and AKT activation (Kharas et al., 2010) in HSCs as well as in myeloid progenitors (Yu et al., 2010) induces myeloproliferative disorder (MPD) and leukemia. Although reduced expression of *TSC* has been reported in a subset of acute leukemia patients (Xu et al., 2009), *Tsc1* loss in HSCs is not sufficient to induce leukemia in mice (Chen et al., 2008). Attenuation of AKT signaling upon *Tsc1/2* disruption might account for the decreased malignant potential of *Tsc1/2*-deficient LGs compared with *Pten* loss, similar to previous reports (Harrington et al., 2004; Manning et al., 2005).

Unexpectedly, both activation and suppression of TORC1 signaling increases the proportion of $PXN^{+}$ cells in the LG at the expense of $dome^{+}$ progenitors. The increased AKT activation that we observe upon conditions of TORC1 pathway suppression, induced via relief of a TOR-dependent negative-feedback loop, may account for the expansion of differentiated hemocytes and CCs observed, although we cannot rule out the possibility that other pathways might contribute to this effect, such as changes in Wingless levels (Shim et al., 2012).

## TORC1-dependent effects of stress and elevated ROS in progenitors

Consistent with the nutrient-sensing function of TOR signaling (Wang and Proud, 2009) and our findings concerning its central role in regulating *Drosophila* hemocyte progenitor proliferation and differentiation, we observed increased differentiation under starvation and low oxygen conditions, which phenocopied reduced TORC1 signaling in the LG. Furthermore, starvation specifically decreased WT LG size (Fig. 7A′), and rearing *Tsc2*-deficient LGs under conditions of starvation rescues their overgrowth, demonstrating the TOR-dependent effects of nutrient availability on proliferation, similar to findings for neural progenitors in *Drosophila* (Sousa-Nunes et al., 2011). An additional metabolic stressor that has been shown to affect LG progenitor differentiation is elevated ROS (Owusu-Ansah and Banerjee, 2009). Manipulation of mitochondrial electron transport chain proteins increases ROS levels in the LG and causes precocious progenitor differentiation, but does not affect tissue size. These effects are not TOR dependent, consistent with their distinct phenotype compared with *Tsc2* and *Pten* disruption. The lack of change in LG size upon rapamycin treatment of *ND42*RNAi larvae is likely to be due to compensatory proliferation of differentiated hemocytes, independent of TOR, which may result from the early loss of progenitors in this background (Owusu-Ansah and Banerjee, 2009). The ROS-dependent LG overgrowth observed upon TORC1 hyperactivation demonstrates mechanistic differences in ROS signaling between conditions of mitochondrial dysfunction and of increased TOR signaling in blood progenitors. Conditional *Tsc1* deletion in mouse HSCs increases ROS, which induces a loss of quiescence and increased cycling that is rescued by decreasing ROS levels (Chen et al., 2008). This and several other studies consistently demonstrated a link between HSC proliferation/quiescence and intracellular oxidation status (Ito et al., 2006; Arai and Suda, 2007; Jang and Sharkis, 2007; Tothova et al., 2007), similar to our findings.

Our results highlight differences in the expansion of intermediate progenitors, differentiated hemocytes and LG-derived circulating hemocytes that are unique to TSC and PTEN, resulting from differential effects on feedback inhibition, AKT activity and autonomous versus non-autonomous TOR activation. We also demonstrate the common effects of *Tsc2* and *Pten* loss on regulating early blood progenitor proliferation in a TORC1-, 4EBP- and ROS-dependent manner and the effects of starvation and hypoxia on TOR-dependent LG growth. This study demonstrates the multifaceted roles of a nutrient-sensing pathway in orchestrating the growth and differentiation of myeloid-specific blood progenitors through regulation of ROS levels and the resulting MPD when dysregulated, highlighting potential non-autonomous effects of *Pten* dysfunction on malignancy.

**Acknowledgements**
We thank N. Perrimon, J. B. Thomas and M. Milan for supplying stocks; and D. Walker, J. Sinsheimer, G. Ferguson, K. Owyang, S. Klein, Y. Tu, T. Munther, S. Ghosh, B. Mondal and J. Shim for technical advice.

**Funding**
This work was supported by a Ruth L. Kirschstein National Research Service Award (NRSA) [GM007185 to M.D.-M.] from the National Institutes of Health, and David Geffen School of Medicine at UCLA (J.A.M.-A.). Deposited in PMC for release after 12 months.

**Competing interests statement**
The authors declare no competing financial interests.

**Supplementary material**
Supplementary material available online at
http://dev.biologists.org/lookup/suppl/doi:10.1242/dev.074203/-/DC1

**References**

**Amcheslavsky, A., Ito, N., Jiang, J. and Ip, Y. T.** (2011). Tuberous sclerosis complex and Myc coordinate the growth and division of Drosophila intestinal stem cells. *J. Cell Biol.* **193**, 695-710.
**Arai, F. and Suda, T.** (2007). Maintenance of quiescent hematopoietic stem cells in the osteoblastic niche. *Ann. N. Y. Acad. Sci.* **1106**, 41-53.
**Castellino, R. C. and Durden, D. L.** (2007). Mechanisms of disease: the PI3K-Akt-PTEN signaling node-an intercept point for the control of angiogenesis in brain tumors. *Nat. Clin. Pract. Neuro.* **3**, 682-693.
**Chen, C., Liu, Y., Liu, R., Ikenoue, T., Guan, K. L., Liu, Y. and Zheng, P.** (2008). TSC-mTOR maintains quiescence and function of hematopoietic stem cells by repressing mitochondrial biogenesis and reactive oxygen species. *J. Exp. Med.* **205**, 2397-2408.
**Evans, C. J. and Banerjee, U.** (2000). Transcriptional regulation of hematopoiesis in Drosophila. *Blood Cells Mol. Dis.* **30**, 223-228.
**Evans, C. J., Hartenstein, V. and Banerjee, U.** (2003). Thicker than blood: conserved mechanisms in Drosophila and vertebrate hematopoiesis. *Dev. Cell* **5**, 673-690.
**Evans, C. J., Olson, J. M., Ngo, K. T., Kim, E., Lee, N. E., Kuoy, E., Patananan, A. N., Sitz, D., Tran, P., Do, M.-T. et al.** (2009). G-TRACE: rapid Gal4-based cell lineage analysis in Drosophila. *Nat. Methods* **6**, 603-605.

**Fingar, D. C., Salama, S., Tsou, C., Harlow, E. and Blenis, J.** (2002). Mammalian cell size is controlled by mTOR and its downstream targets S6K1 and 4EBP1/eIF4E. *Genes Dev.* **16**, 1472-1487.
**Garami, A., Zwartkruis, F. J. T., Nobukuni, T., Joaquin, M., Roccio, M., Stocker, H., Kozma, S. C., Hafen, E., Bos, J. L. and Thomas, G.** (2003). Insulin activation of Rheb, a mediator of mTOR/S6K/4E-BP signaling, is inhibited by TSC1 and 2. *Mol. Cell* **11**, 1457-1466.
**Gingras, A. C., Raught, B. and Sonenberg, N.** (2001). Regulation of translation initiation by FRAP/mTOR. *Genes Dev.* **15**, 807-826.
**Grigorian, M., Mandal, L. and Hartenstein, V.** (2011). Hematopoiesis at the onset of metamorphosis: terminal differentiation and dissociation of the Drosophila lymph gland. *Dev. Genes Evol.* **221**, 121-131.
**Harrington, L. S., Findlay, G. M., Gray, A., Tolkacheva, T., Wigfield, S., Rebholz, H., Barnett, J., Leslie, N. R., Cheng, S., Shepherd, P. R. et al.** (2004). The TSC1-2 tumor suppressor controls insulin-PI3K signaling via regulation of IRS proteins. *J. Cell Biol.* **166**, 213-223.
**Holz, M. K., Ballif, B. A., Gygi, S. P. and Blenis, J.** (2005). mTOR and S6K1 mediate assembly of the translation preinitiation complex through dynamic protein interchange and ordered phosphorylation events. *Cell* **123**, 569-580.
**Inoki, K., Li, Y., Zhu, T., Wu, J. and Guan, K. L.** (2002). TSC2 is phosphorylated and inhibited by Akt and suppresses mTOR signalling. *Nat. Cell Biol.* **4**, 648-657.
**Inoki, K., Li, Y., Xu, T. and Guan, K. L.** (2003). Rheb GTPase is a direct target of TSC2 GAP activity and regulates mTOR signaling. *Genes Dev.* **17**, 1829-1834.
**Ito, K., Hirao, A., Arai, F., Takubo, K., Matsuoka, S., Miyamoto, K., Ohmura, M., Naka, K., Hosokawa, K., Ikeda, Y. et al.** (2006). Reactive oxygen species act through p38 MAPK to limit the lifespan of hematopoietic stem cells. *Nat. Med.* **12**, 446-451.
**Ito, N. and Rubin, G. M.** (1999). gigas, a Drosophila homolog of tuberous sclerosis gene product-2, regulates the cell cycle. *Cell* **96**, 529-539.
**Jang, Y. Y. and Sharkis, S. J.** (2007). A low level of reactive oxygen species selects for primitive hematopoietic stem cells that may reside in the low-oxygenic niche. *Blood* **110**, 3056-3063.
**Jung, S., Evans, C., Uemura, C. and Banerjee, U.** (2005). The Drosophila lymph gland as a developmental model of hematopoiesis. *Development* **132**, 2521-2533.
**Kharas, M. G., Okabe, R., Ganis, J. J., Gozo, M., Khandan, T., Paktinat, M., Gilliland, D. G. and Gritsman, K.** (2010). Constitutively active AKT depletes hematopoietic stem cells and induces leukemia in mice. *Blood* **115**, 1406-1415.
**Kockel, L., Kerr, K. S., Melnick, M., Brückner, K., Hebrok, M. and Perrimon, N.** (2010). Dynamic switch of negative feedback regulation in Drosophila Akt-TOR signaling. *PLoS Genet.* **6**, e1000990.
**Krzemien, J., Dubois, L., Makki, R., Meister, M., Vincent, A. and Crozatier, M.** (2007). Control of blood cell homeostasis in Drosophila larvae by the posterior signalling centre. *Nature* **446**, 325-328.
**Krzemien, J., Oyallon, J., Crozatier, M. and Vincent, A.** (2010). Hematopoietic progenitors and hemocyte lineages in the Drosophila lymph gland. *Dev. Biol.* **346**, 310-319.
**LaFever, L., Feoktistov, A., Hsu, H. J. and Drummond-Barbosa, D.** (2010). Specific roles of Target of rapamycin in the control of stem cells and their progeny in the Drosophila ovary. *Development* **137**, 2117-2126.
**Lanot, R., Zachary, D., Holder, F. and Meister, M.** (2001). Postembryonic hematopoiesis in Drosophila. *Dev. Biol.* **230**, 243-257.
**Lebestky, T., Chang, T., Hartenstein, V. and Banerjee, U.** (2000). Specification of Drosophila hematopoietic lineage by conserved transcription factors. *Science* **288**, 146-149.
**Ma, X. M. and Blenis, J.** (2009). Molecular mechanisms of mTOR-mediated translational control. *Nat. Rev. Mol. Cell Biol.* **10**, 307-318.
**Mandal, L., Martinez-Agosto, J., Evans, C., Hartenstein, V. and Banerjee, U.** (2007). A Hedgehog-and Antennapedia-dependent niche maintains Drosophila haematopoietic precursors. *Nature* **446**, 320-324.
**Manning, B. D., Logsdon, M. N., Lipovsky, A. I., Abbott, D., Kwiatkowski, D. J. and Cantley, L. C.** (2005). Feedback inhibition of Akt signaling limits the growth of tumors lacking Tsc2. *Genes Dev.* **19**, 1773-1778.
**Martinez-Agosto, J. A., Mikkola, H. K. A., Hartenstein, V. and Banerjee, U.** (2007). The hematopoietic stem cell and its niche: a comparative view. *Genes Dev.* **21**, 3044-3060.
**Miron, M., Lasko, P. and Sonenberg, N.** (2003). Signaling from Akt to FRAP/TOR Targets both 4E-BP and S6K in Drosophila melanogaster. *Mol. Cell. Biol.* **23**, 9117-9126.
**Mondal, B. C., Mukherjee, T., Mandal, L., Evans, C. J., Sinenko, S. A., Martinez-Agosto, J. A. and Banerjee, U.** (2011). Interaction between differentiating cell- and niche-derived signals in hematopoietic progenitor maintenance. *Cell* **147**, 1589-1600.
**Owusu-Ansah, E. and Banerjee, U.** (2009). Reactive oxygen species prime Drosophila haematopoietic progenitors for differentiation. *Nature* **461**, 537-541.
**Potter, C. J., Pedraza, L. G. and Xu, T.** (2002). Akt regulates growth by directly phosphorylating Tsc2. *Nat. Cell Biol.* **4**, 658-665.
**Russell, R. C., Fang, C. and Guan, K. L.** (2011). An emerging role for TOR signaling in mammalian tissue and stem cell physiology. *Development* **138**, 3343-3356.
**Shim, J., Mukherjee, T. and Banerjee, U.** (2012). Direct sensing of systemic and nutritional signals by haematopoietic progenitors in Drosophila. *Nat. Cell Biol.* **14**, 394-400.
**Sinenko, S. A., Mandal, L., Martinez-Agosto, J. A. and Banerjee, U.** (2009). Dual role of Wingless signaling in stem-like hematopoietic precursor maintenance in Drosophila. *Dev. Cell* **16**, 756-763.
**Sorrentino, R., Carton, Y. and Govind, S.** (2002). Cellular immune response to parasite infection in the Drosophila lymph gland is developmentally regulated. *Dev. Biol.* **243**, 65-80.
**Sousa-Nunes, R., Yee, L. L. and Gould, A. P.** (2011). Fat cells reactivate quiescent neuroblasts via TOR and glial insulin relays in Drosophila. *Nature* **471**, 508-512.
**Stocker, H., Andjelkovic, M., Oldham, S., Laffargue, M., Wymann, M. P., Hemmings, B. A. and Hafen, E.** (2002). Living with lethal PIP3 levels: viability of flies lacking PTEN restored by a PH domain mutation in Akt/PKB. *Science* **295**, 2088-2091.
**Tapon, N., Ito, N., Dickson, B. J., Treisman, J. E. and Hariharan, I. K.** (2001). The Drosophila tuberous sclerosis complex gene homologs restrict cell growth and cell proliferation. *Cell* **105**, 345-355.
**Tee, A. R., Manning, B. D., Roux, P. P., Cantley, L. C. and Blenis, J.** (2003). Tuberous sclerosis complex gene products, Tuberin and Hamartin, control mTOR signaling by acting as a GTPase-activating protein complex toward Rheb. *Curr. Biol.* **13**, 1259-1268.
**Tothova, Z., Kollipara, R., Huntly, B. J., Lee, B. H., Castrillon, D. H., Cullen, D. E., McDowell, E. P., Lazo-Kallanian, S., Williams, I. R., Sears, C. et al.** (2007). FoxOs are critical mediators of hematopoietic stem cell resistance to physiologic oxidative stress. *Cell* **128**, 325-339.
**Wang, X. and Proud, C. G.** (2009). Nutrient control of TORC1, a cell-cycle regulator. *Trends Cell Biol.* **19**, 260-267.
**Xu, Z., Wang, M., Wang, L., Wang, Y., Zhao, X., Rao, Q. and Wang, J.** (2009). Aberrant expression of TSC2 gene in the newly diagnosed acute leukemia. *Leuk. Res.* **33**, 891-897.
**Yang, Q. and Guan, K. L.** (2007). Expanding mTOR signaling. *Cell Res.* **17**, 666-681.
**Yilmaz, O. H., Valdez, R., Theisen, B. K., Guo, W., Ferguson, D. O., Wu, H. and Morrison, S. J.** (2006). Pten dependence distinguishes haematopoietic stem cells from leukaemia-initiating cells. *Nature* **441**, 475-482.
**Yu, H., Li, Y., Gao, C., Fabien, L., Jia, Y., Lu, J., Silberstein, L. E., Pinkus, G. S., Ye, K., Chai, L. et al.** (2010). Relevant mouse model for human monocytic leukemia through Cre/lox-controlled myeloid-specific deletion of PTEN. *Leukemia* **24**, 1077-1080.
**Zhang, J., Grindley, J. C., Yin, T., Jayasinghe, S., He, X. C., Ross, J. T., Haug, J. S., Rupp, D., Porter-Westpfahl, K. S., Wiedemann, L. M. et al.** (2006). PTEN maintains haematopoietic stem cells and acts in lineage choice and leukaemia prevention. *Nature* **441**, 518-522.

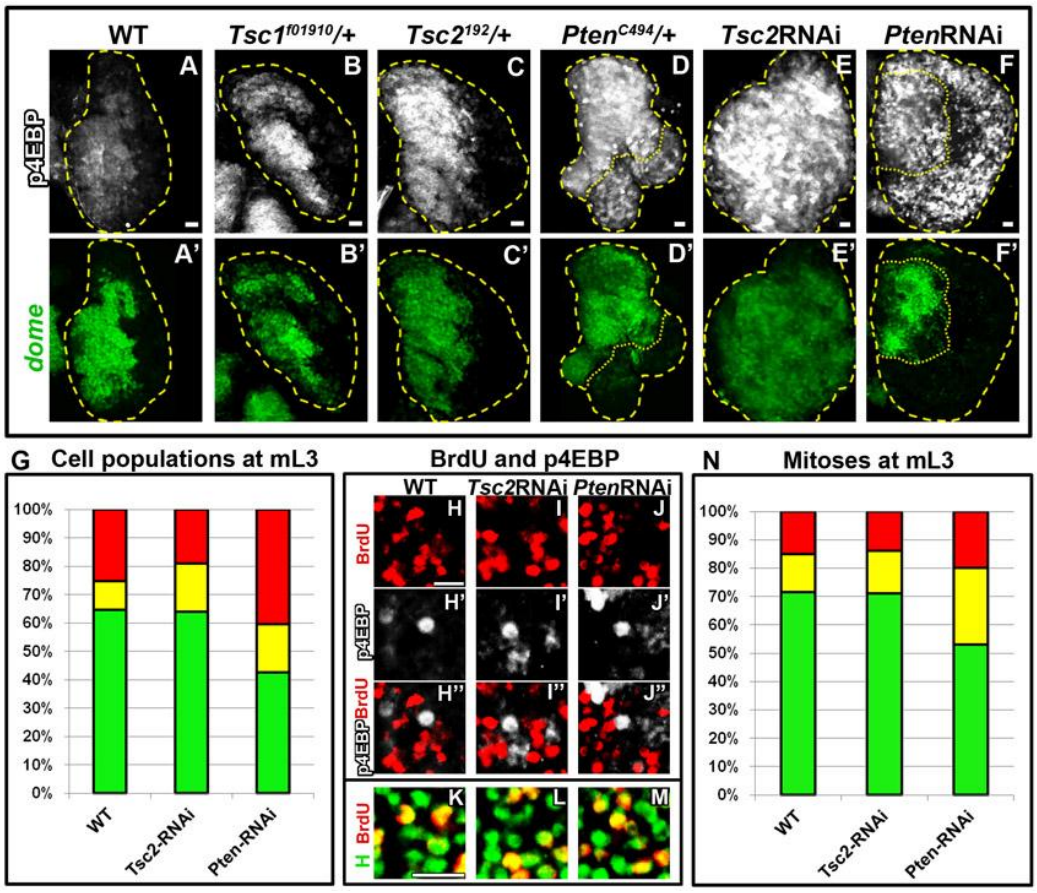


**Fig. S1. Expression of p4EBP, cell population distributions and mitoses upon disruption of *Tsc1/2* and *Pten* function.** (**A-F9**) Increase in p4EBP expression upon TORC1 pathway manipulation at wL3. Single-copy loss of *Tsc1* (*Tsc1*$^{f01910}$/+) (B,B9) or *Tsc2* (*Tsc2*$^{192}$/+) (C,C9) increases p4EBP expression (white) in *dome*$^{+}$ hemocyte progenitors (green), compared with WT (A,A9). Single-copy loss of *Pten* (*Pten*$^{C494}$/+) (D,D9) increases p4EBP expression both within *dome*$^{+}$ and *dome*$^{-}$ hemocytes. Downregulation of *Tsc2* (*dome*>*Tsc2*RNAi; E,E9) in hemocyte progenitors autonomously increases p4EBP expression in *dome*$^{low}$ hemocytes throughout the LG. Downregulation of *Pten* (*dome*>*Pten*RNAi, F,F9) increases p4EBP autonomously within *dome*$^{+}$ hemocytes and non-cell-autonomously in *dome*-negative hemocytes. (**G**) Hemocyte and progenitor cell distributions at mL3 among the populations of *dome*$^{+}$/PXN$^{-}$ prohemocytes (PH, green), *dome*$^{+}$/PXN$^{+}$ intermediate progenitors (IP, yellow), and *dome*$^{-}$/PXN$^{+}$ differentiated hemocytes (DH, red). WT LGs are composed of 65±5% PH, 10±3% IP and 25±5% DH. *Tsc2* downregulation in progenitors does not affect prohemocyte population size at mL3: 64±5% of the LG represents PH, whereas 17±3% of cells are IP and 19±6% are DH. *Pten* deficiency increases differentiation at the cost of prohemocytes: 43±8% of the LG represents PH, whereas 17±4% are IP and 40±9% are DH. Data are mean ± s.d. (*n*=10). Two-way ANOVA statistics showed significant changes (*P*<0.0001) in the distribution of hemocyte populations in *Tsc2*- or *Pten*-deficient LGs compared with WT at mL3. (**H-M**) Bromodeoxyuridine (BrdU, red) incorporation in WT (*dome*>*gal4*) (H-H0,K), *dome*>*Tsc2*RNAi (I-I0,L) and *dome*>*Pten*RNAi (J-J0,M) LGs at eL2. BrdU, a marker of cells in S phase, does not colocalize with p4EBP$^{high}$ cells in any backgrounds (H-J0). Histone (H, green), a nuclear marker, overlaps with BrdU (red), indicating nuclear localization of BrdU (K-M). (**N**) Distribution of mitoses in mL3 LGs among the populations of *dome*$^{+}$/PXN$^{-}$ prohemocytes (PH, green), *dome*$^{+}$/PXN$^{+}$ intermediate progenitors (IP, yellow) and *dome*$^{-}$/PXN$^{+}$ differentiated hemocytes (DH, red). In WT, 71.5±1.8% of mitoses occur in PH, whereas 13.5±3.4% occur in IP and 15±2.5% in DH. *Tsc2* downregulation does not affect the proportion of mitoses that occur in PH: 71±6.6% of mitoses occur within PH, whereas 15±5.3% occur in IP and 13.9±5.3% of mitoses occur in DH. By contrast, *Pten* downregulation decreases the proportion of mitoses in PH to 53.1±5.8%, whereas 27.1±5.3% of mitoses occur in IP and 19.8±7% in DH. Data are mean ± s.d. (*n*=10). Two-way ANOVA statistics comparing the distribution of mitoses at mL3 in *Tsc2*- and *Pten*-deficient LGs compared with WT showed no difference for *Tsc2*RNAi LGs (*P*>0.05), but a significant change upon *Pten* deficiency (*P*<0.0001). Scale bars: 20 μm in A-F; 10 μm in H-M.

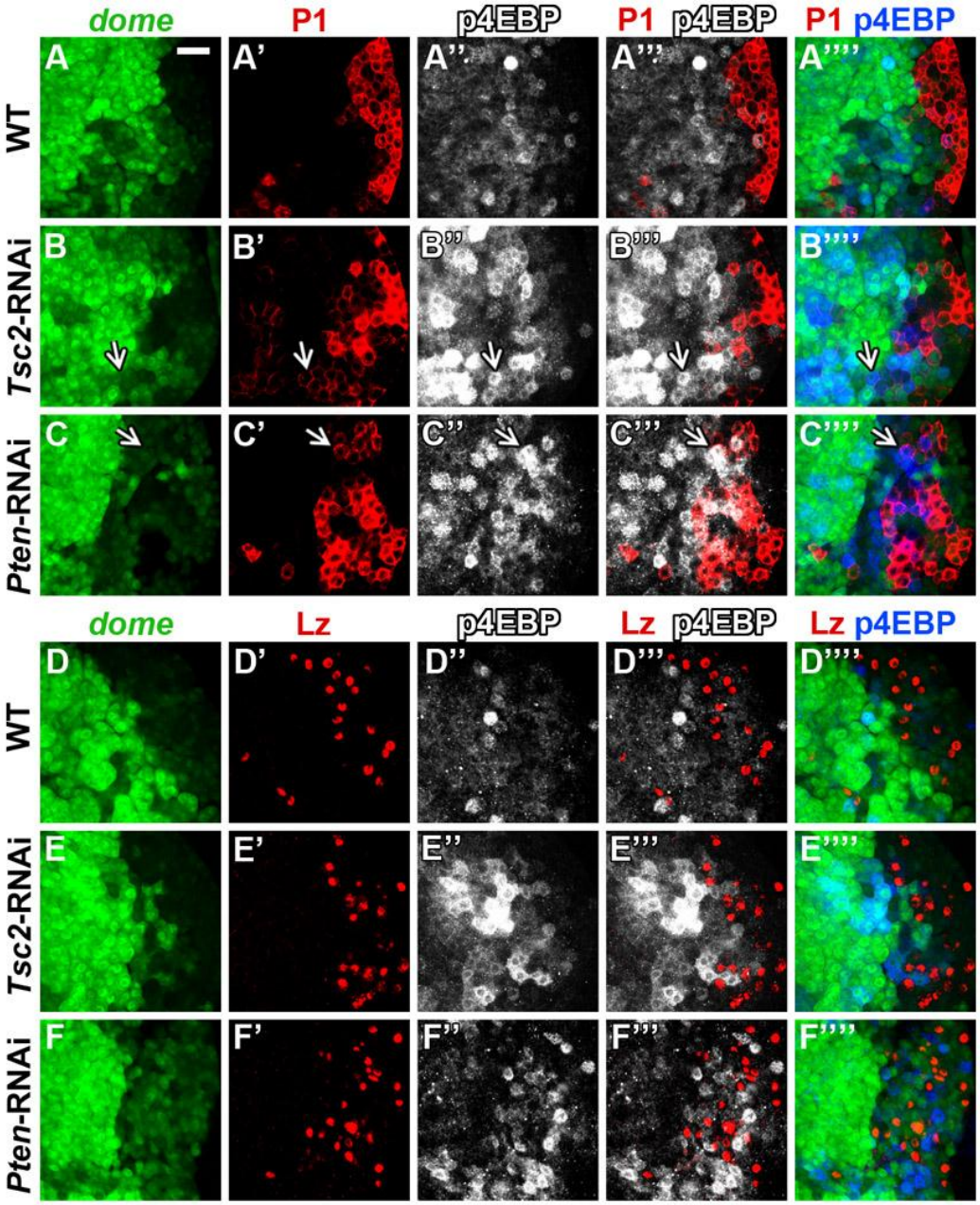


**Fig. S2. Distribution of p4EBP$^{high}$ cells in *Tsc2*- and *Pten*-deficient LGs at mL3.** All panels represent mL3 LGs. p4EBP is shown in white in columns 3 and 4 and in blue in column 5. P1 (A-C−9) labels differentiated PLs, and LZ (D-F−9) labels CCs and their progenitors. L1$^{+}$ lamellocytes were not observed at this stage in any of the genetic backgrounds. (**A-A-9**,**D-D-9**) WT. p4EBP is expressed throughout the primary lobe at low levels with some scattered p4EBP$^{high}$ cells. A small population of P1$^{+}$ (A-A−9) and LZ$^{+}$ (D-D−9) hemocytes is present. (**B-B-9**,**E-E-9**) Downregulation of *Tsc2* (*dome*>*Tsc2*RNAi) expands the population of p4EBP$^{high}$ cells. Rare p4EBP$^{high}$ cells colocalize with P1$^{low}$ (B-B−9) hemocytes (arrows), but not with P1$^{high}$ hemocytes or with LZ$^{+}$ cells (E-E−9). (**C-C-9**,**F-F-9**) Downregulation of *Pten* (*dome*>*Pten*RNAi) expands the population of p4EBP$^{high}$ cells. A subset of P1$^{+}$ hemocytes (arrows, C-C−9) are p4EBP$^{high}$, including some P1$^{high}$ cells. LZ$^{+}$ cells are often observed adjacent to p4EBP$^{high}$ cells but they do not overlap (F-F−9). Scale bar: 20 μm.

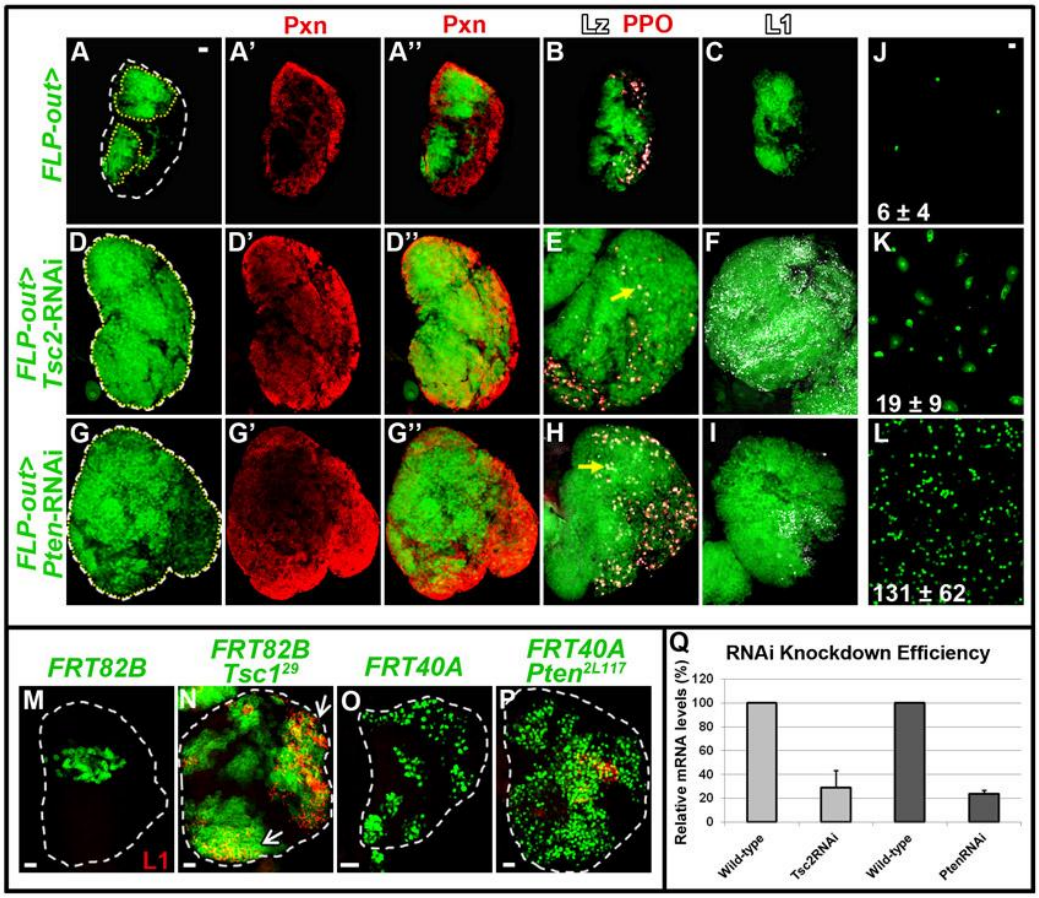


**Fig. S3. Clonal analysis and knockdown efficiencies of *Tsc2*RNAi and *Pten*RNAi.** Clones are demarcated in yellow in A,D,G. (**A-C**) WT LGs (*FLP-out*>): clonal expression of GFP (green) and normal expression of differentiation markers PXN (red, A9,A0), PPO (red, B), LZ (white, B) and L1 (white, C; not normally present in WT). (**D-F**) Clonal expression of *Tsc2*RNAi (*FLP-out*>*Tsc2*RNAi) increases LG size and GFP-marked clones encompass the entire LG lobe (compare with A-C). PXN (D9,D0) and L1 (F) expression expands throughout the LG. A small number of $LZ^{+}/PPO^{-}$ CC progenitors (arrow) are also seen in medial regions of the LG (E), unlike in WT. (**G-I**) Clonal expression of *Pten*RNAi (*FLP-out*>*Tsc2*RNAi) increases LG size and increases differentiation (G9-H) with few lamellocytes observed (I). (**J-L**) Hemocyte bleeds from LG-specific lineage-traced larvae. GFP marks hemocytes in circulation that are derived from the LG. Very few LG-derived $GFP^{+}$ hemocytes are observed in circulation in WT (J). Downregulation of *Tsc2* in the LG induces the release of LG-derived hemocytes, particularly lamellocytes, into circulation (K). Downregulation of *Pten* in the LG increases the relative number of LG-derived hemocytes, but not lamellocytes, released into circulation (L) compared with WT ($P<0.001$; J) or *Tsc2* downregulation ($P<0.001$; K). Data are mean ± s.d., $n=10$. (**M-P**) All panels represent wL3. MARCM clones for WT [*hs-flp FRT82B Tub-mCD8-GFP* (M) and *hs-flp FRT40A Tub-nGFP* (O)], $Tsc1^{29}$ (*hs-flp FRT82B* $Tsc1^{29}$ *FRT82B Tub-mCD8-GFP*, N) and $Pten^{2L117}$ (*hs-flp FRT40A* $Pten^{2L117}$ *FRT40A Tub-nGFP*, P). In WT, lamellocytes (red) are not observed (M,O). $Tsc1^{-/-}$ clones autonomously induce lamellocyte differentiation (arrows, N). $Pten^{-/-}$ clones induce a small number of lamellocytes (P). (**Q**) Knockdown efficiency of *Tsc2*RNAi and *Pten*RNAi constructs. Quantitative RT-PCR was performed to assess the relative levels of *Tsc2* or *Pten* at wL3, following ubiquitous expression of their respective RNAi constructs with *daughterless-Gal4*. Data are the mean of three replicates ± s.d. *Tsc2* mRNA transcripts were detected at 29.02% of WT, and *Pten* mRNA transcripts were detected at 23.88% of WT. Scale bars: 20 μm; except for 1.23 magnification for I.

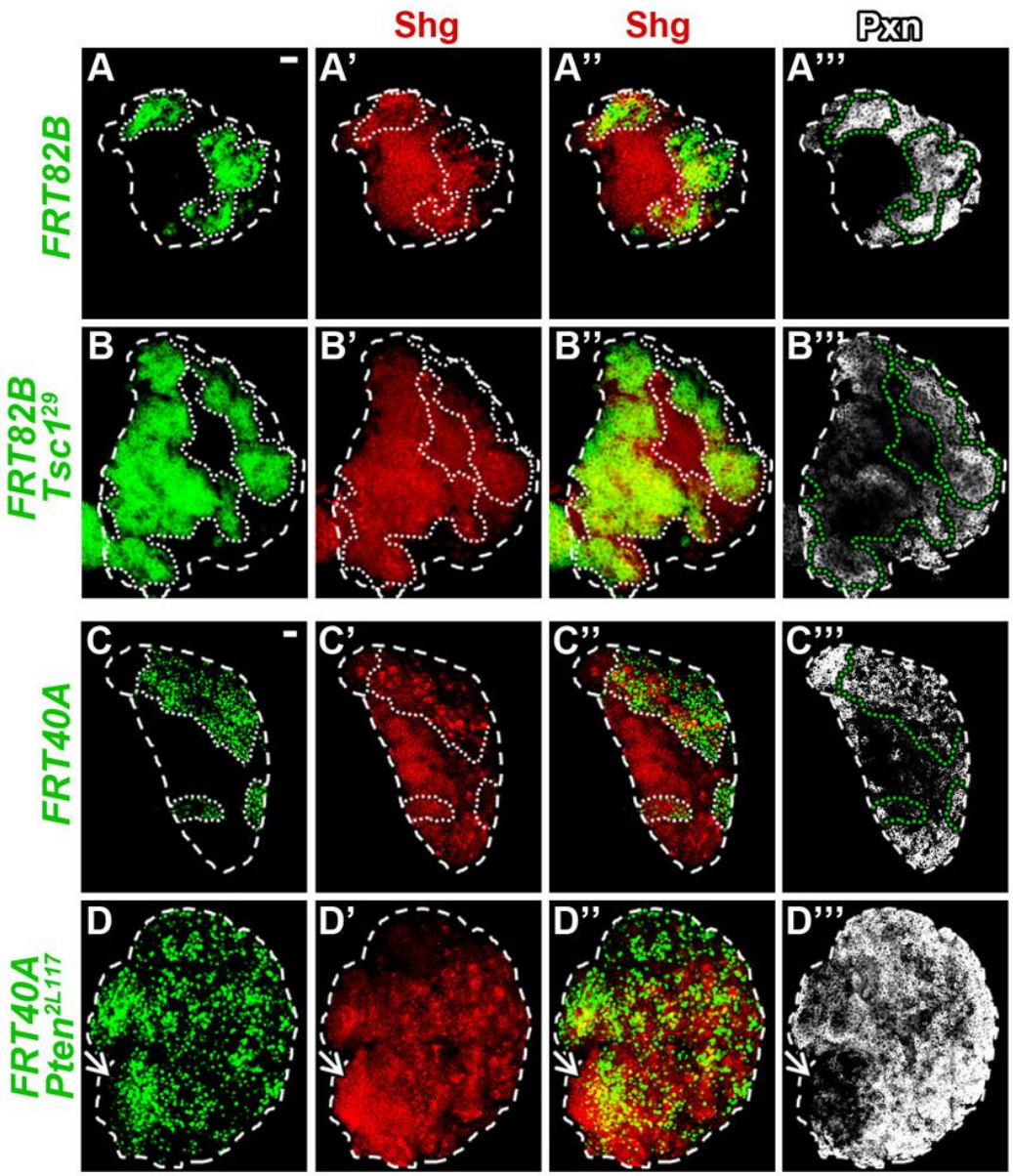


**Fig. S4. Shotgun expression in *Tsc1* and *Pten* LOF backgrounds.** All panels represent wL3. Clones are outlined by a white or green dotted line. (**A-B-**) *Tsc* MARCM clones. (A-A−) WT MARCM clones (*hs-flp FRT82B Tub-mCD8-GFP*). (B-B−) $Tsc1^{29}$ clones (*hs-flp FRT82B* $Tsc1^{29}$ *FRT82B Tub-mCD8-GFP*) maintain Shotgun (SHG, DE-cadherin) expression (red) in $Tsc1^{-/-}$ clones (green). High PXN expression (white) is observed only at the tissue periphery, while $Tsc1^{-/-}$ cells express low PXN levels (gray, B−). (**C-D-**) *Pten* MARCM clones. (C-C−) WT MARCM clones (*hs-flp FRT40A Tub-nGFP*) express highest SHG expression in medial, PXN-negative tissue. Cells in the periphery are differentiated and express reduced SHG levels, except for non-specific expression of SHG in scattered cells. (D-D−) $Pten^{2L117}$ clones (*hs-flp FRT40A* $Pten^{2L117}$ *FRT40A Tub-nGFP*) that are medially localized (arrow) are PXN negative and express high SHG levels. Scattered $Pten^{-/-}$ cells in the periphery are $PXN^{high}$ (white) and express reduced levels of SHG, except for some scattered cells. Scale bars: 20 μm.

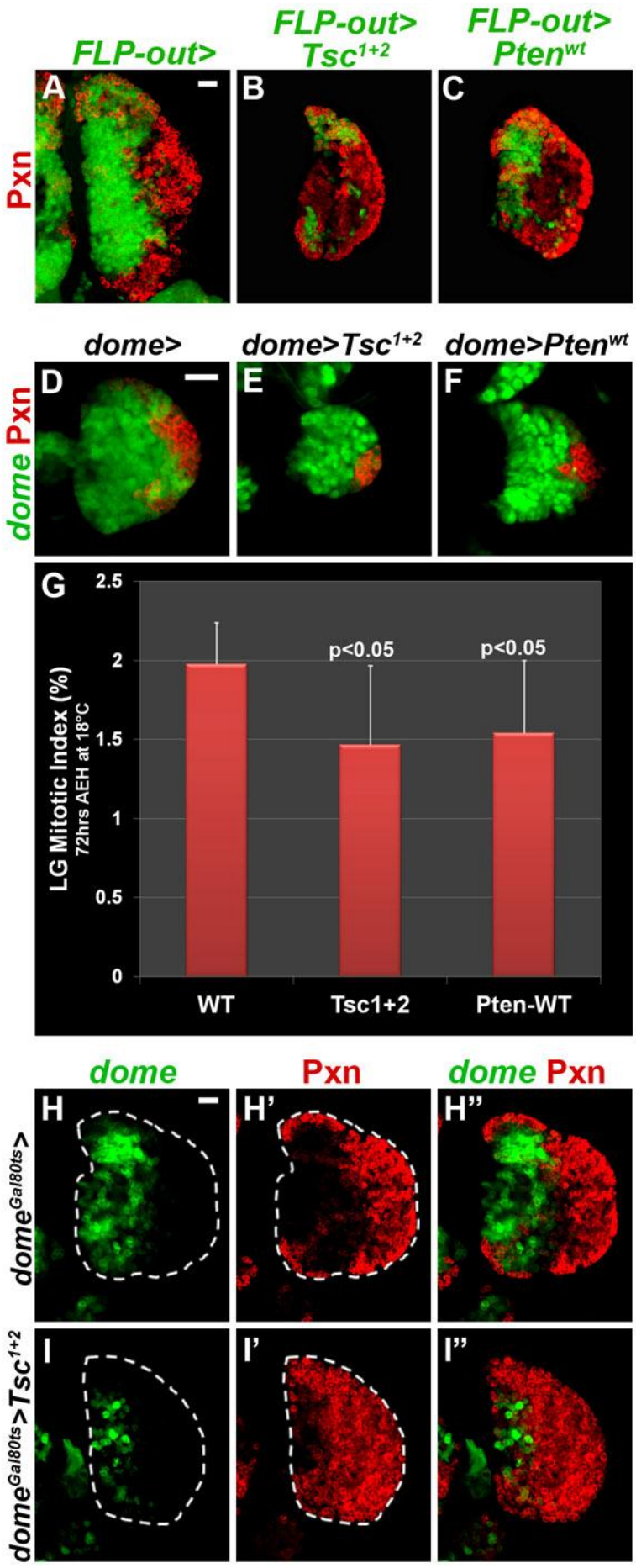
FLP-out>
FLP-out> Tsc1+2
FLP-out> Pten^wt
A
B
C
Pxn
dome>
dome>Tsc1+2
dome>Pten^wt
D
E
F
dome Pxn
G
LG Mitotic Index (%)
72hrs AEH at 18°C
2.5
2
1.5
1
0.5
0
p<0.05
p<0.05
WT
Tsc1+2
Pten-WT
dome
Pxn
dome Pxn
H
H'
H"
dome^Gal80ts>
I
I'
I"
dome^Gal80ts>Tsc1+2

**Fig. S5. Inhibition of TORC1 signaling in prohemocytes impairs early LG growth.** (**A-C**) FLP-out clones were generated specifically in the LG for WT (*FLP-out>*; A), $Tsc^{1+2}$ (*FLP-out> $Tsc^{1+2}$*; B) and $Pten^{wt}$ (*FLP-out> $Pten^{wt}$*; C). Clonal overexpression of $Tsc^{1+2}$ (B) or $Pten^{wt}$ (C) reduces overall LG size at wL3 and increases the population of $PXN^+$ hemocytes (red). (**D-F**) Overexpression of $Tsc^{1+2}$ (E) and $Pten^{wt}$ (F) in prohemocytes decreases overall LG size at lL2, compared with WT (*dome>*, D), but the onset of differentiation of a small number of $PXN^+$ (red) hemocytes at the LG periphery occurs normally. Staging of *dome>$Tsc^{1+2}$* and *dome>$Pten^{wt}$* was performed at 18°C and lL2 larvae were dissected at 72 hours AEH. (**G**) Quantification of mitotic index at lL2. Overexpression of $Tsc^{1+2}$ (1.47±0.5%, $P<0.0001$) or $Pten^{wt}$ (1.54±0.46, $P<0.0001$) in prohemocytes decreases mitotic index, compared with WT (1.98±0.26%). Data are mean ± s.d., $n=10$. (**H-I0**) Delaying expression of $Tsc^{1+2}$ in prohemocytes until eL3 does not alter LG size (compare I0 with H0) but increases the number of $PXN^+$ differentiated hemocytes (red). Late expression of *UAS-$Tsc^{1+2}$* in progenitors was induced using *dome-gal4; P{tubP-gal80[ts]}20* and shifting larvae to the restrictive temperature (29°C) at eL3. Scale bars: 20 μm (for each row).

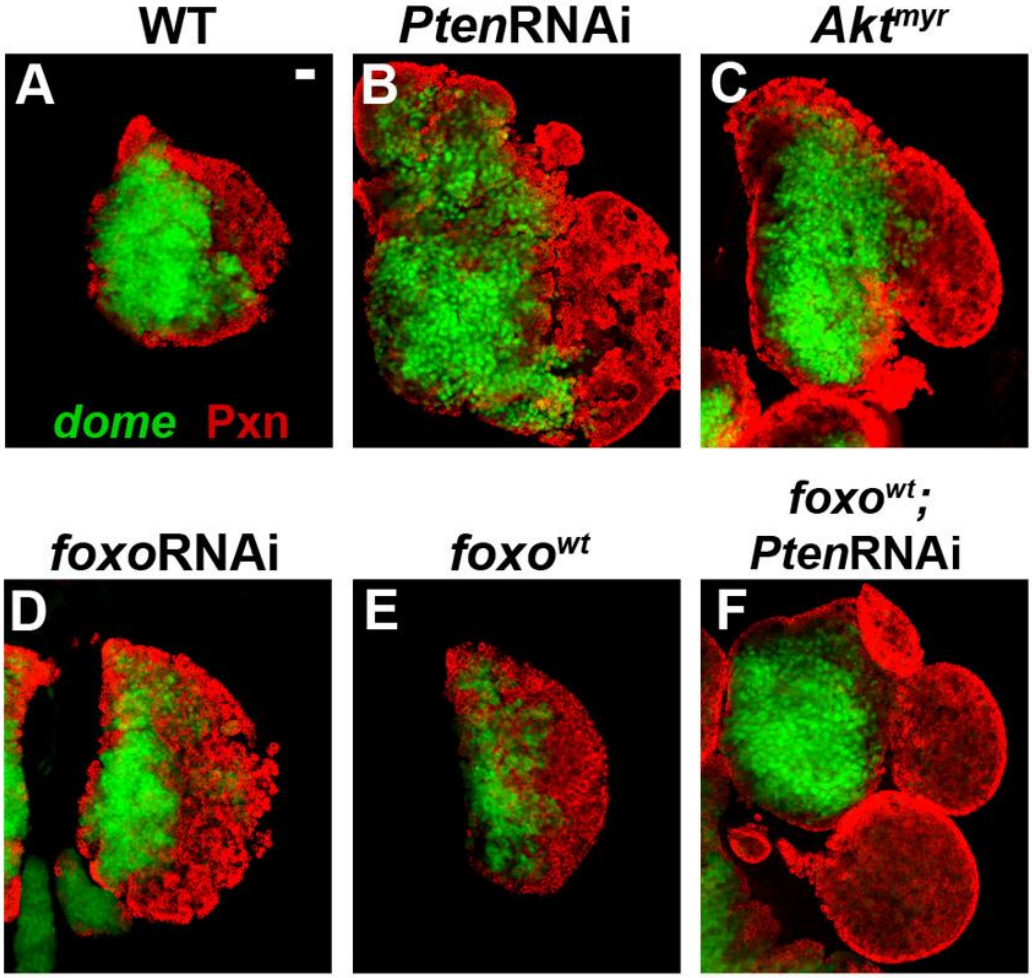


**Fig. S6. FOXO-independent role of AKT in mediating *Pten* LOF phenotypes.** All panels represent wL3 LGs. In all panels, *dome-gal4, UAS-2xEGFP* (green) drives expression of the genetic constructs listed. PXN expression is in red. (**A**) WT LG. (**B**) *Pten* downregulation in prohemocytes increases LG size and expands the population of $PXN^+$ hemocytes. (**C**) Overexpression of activated *Akt* (*$Akt^{myr}$*) increases the population of $PXN^+$ hemocytes, which sometimes 'bud' at the LG periphery. (**D**) Downregulation of *foxo* in prohemocytes does not phenocopy *$Akt^{myr}$* overexpression (C) or *Pten* downregulation (B) in the LG. (**E**) Overexpression of *foxo* increases $PXN^+$ hemocytes at the expense of prohemocytes. (**F**) Overexpression of *foxo* upon *Pten* downregulation does not rescue the accumulation of differentiated hemocytes associated with *Pten* deficiency (B). Scale bar: 20 μm.